J. Fluid Mech. (1991), *vol.* 227, *pp.* 587–615
Printed in Great Britain

Lubricated pipelining: stability of core–annular flow. Part 4. Ginzburg–Landau equations

By KANGPING CHEN[1] AND DANIEL D. JOSEPH[2]

[1] Department of Mechanical and Aeronautical Engineering, Clarkson University, Potsdam, NY 13676, USA

[2] Department of Aerospace Engineering and Mechanics, University of Minnesota, Minneapolis, MN 55455, USA

(Received 19 February 1990 and in revised form 19 September 1990)

Nonlinear stability of core–annular flow near points of the neutral curves at which perfect core–annular flow loses stability is studied using Ginzburg–Landau equations. Most of the core–annular flows are always unstable. Therefore the set of core–annular flows having critical Reynolds numbers is small, so that the set of flows for which our analysis applies is small. An efficient and accurate algorithm for computing all the coefficients of the Ginzburg–Landau equation is implemented. The nonlinear flows seen in the experiments do not appear to be modulations of monochromatic waves, and we see no evidence for soliton-like structures. We explore the bifurcation structure of finite-amplitude monochromatic waves at criticality. The bifurcation theory is consistent with observations in some of the flow cases to which it applies and is not inconsistent in the other cases.

1. Introduction

This paper is a continuation of the study of the stability of water-lubricated core–annular flows. In the previous studies, Joseph, Renardy & Renardy (1984), Preziosi, Chen & Joseph (1989, hereinafter referred to as PCJ), Hu & Joseph (1989, hereinafter referred to as HJ), Chen, Bai & Joseph (1990, hereinafter referred to as CBJ), and more recently Bai, Chen & Joseph (1991, hereinafter referred to as BCJ), calculations from the linear theory of stability were reported and compared with experiments. Surprisingly, the linear theory turned out to be good for predicting wavelengths, wave speeds and flow types in flows which are far from the perfect core–annular state (which the linear theory is supposed to perturb only slightly). However, there are some situations for which the linear theory fails, and it is of interest here to see what understanding can be achieved from nonlinear theory. One such situation mentioned by BCJ is a regime in which oil seizes the pipe wall. Efforts are also made here to correlate the 'bamboo' waves, shown in figure 1, which are the dominant flow regime in up-flow, to the weakly nonlinear analysis. Unfortunately, it is found that these waves cannot be obtained from this theory.

The first type of nonlinear analysis we might try is bifurcation theory. This theory, however, is restricted in applications to those cases in which there is a threshold for instability; in our situation this means cases in which stable PCAF (perfect core–annular flow) is possible (the neutral curves are separated as in figures 3 and 4). In these cases we may go beyond bifurcation into monochromatic waves and derive amplitude equations which allow for slow modulations of wavy flow in space and

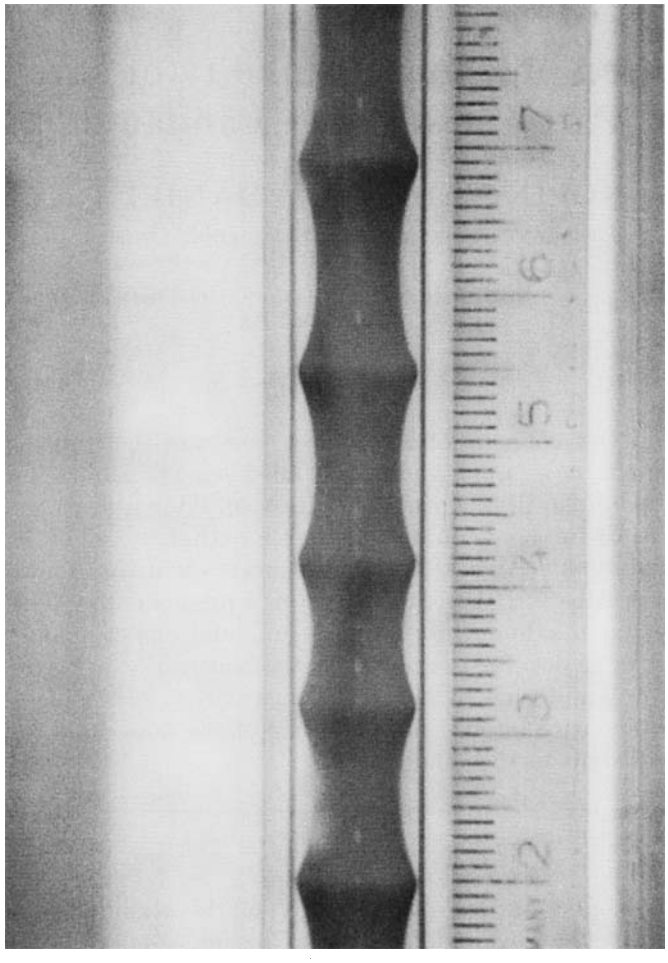

FIGURE 1. Bamboo waves observed in up-flows of motor oil and water. The oil has a viscosity of 13.32 poise and a density of 0.881 g/cm^3 at room temperature $T = 22$ °C. The volume flow rates are $Q_o = 0.11332$ GPM, $Q_w = 0.05284$ GPM (from BCJ 1990).

time. This amplitude equation is called the Ginzburg–Landau equation.† There are many regimes of flow which give rise to separated neutral curves for which Ginzburg–Landau equation may be applied. There are even more regimes in which PCAF is not possible and analytical approaches to the nonlinear problem in these cases seem to be unknown. The neutral curves shown in figures 10 and 14 of PCJ and figure 19 of CBJ where the upper and the lower branches have merged to form left and right branches, will not allow for bifurcation analysis. Unfortunately, the case $m \ll 1$ which is typical of applications in which the oil is very viscous is one of these cases (see Hu, Lundgren & Joseph 1990, hereinafter referred to as HLJ).

Amplitude equations are derived under restricted conditions. Once derived, they take on a life of their own and may be applied in all sorts of situations for which they

† The so-called 'Ginzburg–Landau' equation which we derive actually follows the work of Newell (1974) and Stewartson & Stuart (1971) who extended the work of Newell & Whitehead (1969) and Segel (1969) to the unsteady case in which the marginally stable eigenvalue at criticality is purely imaginary, as in Hopf bifurcation. Ginzburg & Landau (1950) did write down, but did not derive a differential amplitude equation with slow modulation for the theory of superconductivity.

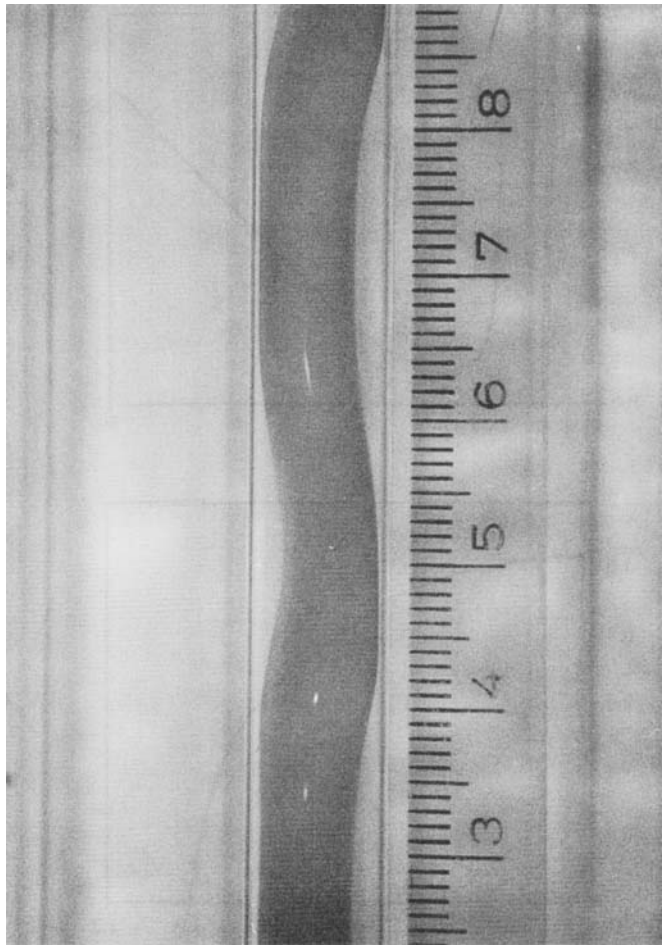

FIGURE 2. Corkscrew waves observed in down-flows of motor oil and water. The oil has a viscosity of 13.32 poise and a density of 0.881 g/cm^3 at room temperature $T = 22$ °C. The volume rates are $Q_o = 0.08212$ GPM, $Q_w = 0.05284$ GPM (from BCJ 1990).

were never intended. For example, the Ginzburg–Landau equation presumably applies only to small-amplitude waves which modulate a monochromatic wave of wavelength $2\pi/\alpha_c$, where α_c is the critical wavenumber at the nose of the neutral curve. A modulated wave solving the Ginzburg–Landau equation (3.12) has a slowly varying amplitude $A(\xi,\tau), \xi = \epsilon(x-c_g t), \tau = \epsilon^2 t$ (see (3.3)), where ϵ (given by (3.1)) is small and determines the bandwidth of excited waves centred on the wavelength $2\pi/\alpha_c$ of the monochromatic wave. $A(\xi,\tau)$ is the envelope of amplitudes of this modulated wave. The length of an A wave may be computed from the Ginzburg–Landau equation. It is of interest to see what kinds of effects may be described by solutions lying in the full solution set of Ginzburg–Landau equations. The formation of solitons and chaos are two such effects which have been examined in a qualitative way in the works of Moon, Huerre & Redekopp (1983) and Bretherton & Spiegel (1983). There are many recent works on defects in which the coefficients of the Ginzburg–Landau equations are selected so as to give apparent agreement between computer simulations and experiments. Obviously such qualitative studies go only part of the way, perhaps not even a part. What we need

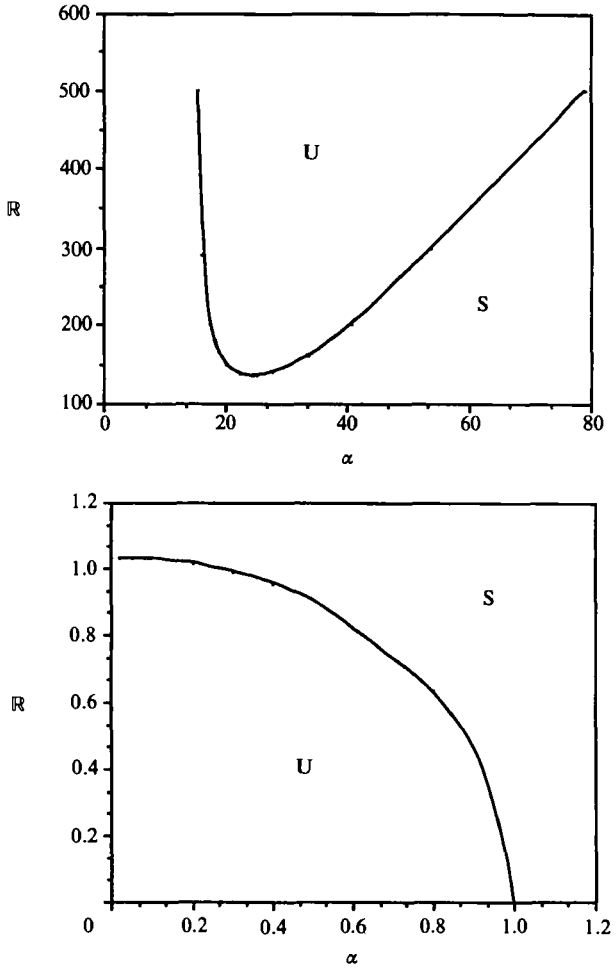

FIGURE 3. Neutral curves for $a = 1.1$, $m = 0.5$, $\zeta_2 = 1.2$, $J^* = 1.0$, $\mathbb{R}_g = 0.5$, down-flow. 'U' and 'S' stand for 'unstable' and 'stable'. The upper and the lower branches are well separated. surface tension is weak and the critical Reynolds number for the lower branch occurs at $\alpha = 0.09$.

are the explicit coefficients for the Ginzburg–Landau equation which applies to the experiment. With this information, we may hope to answer the question 'where is the modulation', and to look for structures which can be described as modulations of monochromatic waves.

In this paper, we have computed the coefficients of the Ginzburg–Landau equations for different situations of interest and we make some comparisons with experiments. We have adopted an efficient numerical method, the singular value decomposition (SVD), to problems of bifurcation. SVD is the method of choice for the computation of the coefficients of amplitude equations and normal forms. This method is fully described in §4. Our comparison of Ginzburg–Landau theory with experiments is limited by the fact that the theory only applies to the small set of situations in which there are stable flows. Even in these cases, we see no evidence for modulations, so that our calculations are rather more in the way of an application of Ginzburg–Landau equations to the bifurcation of nonlinear monochromatic waves than to any kind of modulation of these waves. In this restricted application, we do see some agreement between the weakly nonlinear theory and experiment. In the

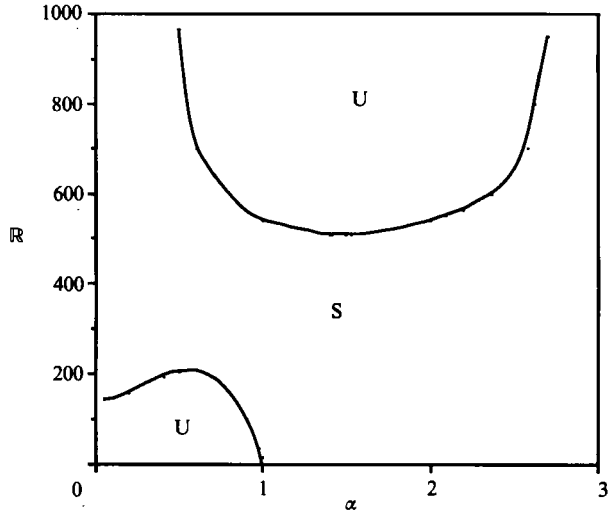

FIGURE 4. Neutral curves for $a = 1.3$, $m = 0.5$, $\zeta_2 = 1.2$, $J^* = 2000$, $\mathbb{R}_g = 0.5$, down-flow. 'U' and 'S' stand for 'unstable' and 'stable'. For this case of strong surface tension, the critical Reynolds number for the lower branch occurs at a finite wavenumber $\alpha = 0.56$.

problem of water-lubricated pipelining, we have so far obtained many useful results from the study of the linearized theory of stability, with only limited success from nonlinear theories.

2. Nonlinear evolution of axisymmetric disturbances in core–annular flows

Two immiscible fluids are flowing inside a pipe of radius R_2. The interface between the two fluids is perfectly cylindrical, $r = R_1$. Fluid 1 is located in the core and fluid 2 in the annulus. We are interested in the stability of this core–annular flow.

It was shown by PCJ and CBJ that there are five independent controlling parameters: a, m, ζ_2, J^* and $\mathbb{R}_1$ for horizontal core–annular flow and six for vertical core–annular flow: a, m, ζ_2, J^*, $\mathbb{R}_g$ and F (defined below). Although a multi-parameter bifurcation analysis is possible, we restrict here our attention to the simplest case in which a single parameter is varied for fixed values of the other five. We prefer a parameter that we control in our experiments once the working fluids and the pipe are chosen. For horizontal flow, the Reynolds number $\mathbb{R}_1$ defined in PCJ can be used as the bifurcation parameter. For vertical flow, however, the Reynolds number defined in CBJ is based on gravity and is more like a geometrical than a dynamical parameter. A better dynamical parameter is the forcing ratio $F = f/\rho_1 g$, where $f = -\mathrm{d}\hat{P}_1/\mathrm{d}x = -\mathrm{d}\hat{P}_2/\mathrm{d}x$ is the applied pressure gradient. In this paper we shall use a different equivalent set of parameters incorporating both horizontal and vertical flows.

We shall choose the magnitude of the centreline velocity $|W(0)|$ as the velocity scale, R_1 the lengthscale and $R_1/|W(0)|$ the timescale. We define the following parameters:

$$a = \frac{R_2}{R_1},$$

$$(m_1, m_2) = (1, m) = \left(1, \frac{\mu_2}{\mu_1}\right),$$

$$(\zeta_1, \zeta_2) = (1, \zeta) = \left(1, \frac{\rho_2}{\rho_1}\right),$$

$$\mathbb{R} \overset{\text{def.}}{=} \mathbb{R}_1 = \frac{|W(0)|\rho_1 R_1}{\mu_1} \quad \text{(Reynolds number)},$$

$$\mathbb{R}_2 = \frac{|W(0)|\rho_2 R_1}{\mu_2} = \frac{\zeta_2}{m}\mathbb{R},$$

$$\mathbb{R}_g = \frac{gR_2^3}{\nu_1^2} = \frac{gR_1^3 a^3}{\nu_1^2} \quad \text{(Reynolds number based on gravity.}$$

This is different to $\mathbb{R}_g = \left(\frac{gR_1^3}{\nu_1^2}\right)^{\frac{1}{2}}$ used by CBJ.)

$$J^* = \frac{TR_2}{\rho_1 \nu_1^2},$$

$$\mathbb{K} = \frac{f+\rho_1 g}{f+\rho_2 g} \quad \text{(ratio of driving forces in core and annulus)},$$

where (μ, ρ, ν, g, T) = (viscosity, density, μ/ρ, gravity, interfacial tension),

subscripts 1 and 2 refer to fluids 1 and 2 respectively, and f is one and the same constant for both core and annulus. The cylindrical polar coordinate system is chosen such that gravity is acting in the positive x-direction. We choose the Reynolds number $\mathbb{R}$ as our bifurcation parameter. When the density is matched, $\mathbb{K} = 1$ and gravity does not enter the problem. $\mathbb{R}_g, J^*$ are known constants once the working fluids and pipe radius are given, independent of flow conditions.

The basic flow in dimensional form is given in (2.2) of CBJ. The velocity at the centreline of the pipe is

$$W(0) = \frac{f+\rho_1 g}{4\mu_1} R_1^2 + \frac{f+\rho_2 g}{4\mu_2}(R_2^2 - R_1^2) + \frac{[\![\rho]\!] g R_1^2}{2\mu_2} \ln \frac{R_2}{R_1}.$$

Using this relation we can show that the parameter $\mathbb{K}$ can be expressed in terms of $\mathbb{R}_g$ and $\mathbb{R}$. To do this we need to distinguish between the cases $W(0) > 0$ and $W(0) < 0$. For convenience, we will loosely refer to flows with $W(0) > 0$ as down-flows and $W(0) < 0$ as up-flows, although mixed flows are also possible for both cases, depending on the magnitude of $W(0)$ or f, as shown in CBJ. Then the dimensionless basic flow can be expressed as:

(*a*) down-flow: $W(0) > 0$

$$\mathbb{K}(\mathbb{R}) = \frac{4ma^3 \mathbb{R} + [\![\zeta]\!] \mathbb{R}_g (a^2 - 1 - 2\ln a)}{4ma^3 \mathbb{R} - [\![\zeta]\!] \mathbb{R}_g (m + 2\ln a)}, \tag{2.1a}$$

$$W_1(r, \mathbb{R}) = 1 - \frac{m\mathbb{K}(\mathbb{R}) r^2}{m\mathbb{K}(\mathbb{R}) + a^2 - 1 + 2(\mathbb{K}(\mathbb{R}) - 1)\ln a} \quad (0 \leqslant r \leqslant 1), \tag{2.1b}$$

$$W_2(r, \mathbb{R}) = \frac{a^2 - r^2 - 2(\mathbb{K}(\mathbb{R}) - 1)\ln \frac{r}{a}}{m\mathbb{K}(\mathbb{R}) + a^2 - 1 + 2(\mathbb{K}(\mathbb{R}) - 1)\ln a} \quad (1 \leqslant r \leqslant a). \tag{2.1c}$$

(*b*) up-flow: $W(0) < 0$

$$\mathbb{K}(\mathbb{R}) = \frac{4ma^3\,\mathbb{R} - [\![\zeta]\!]\,\mathbb{R}_g(a^2-1-2\ln a)}{4ma^3\,\mathbb{R} + [\![\zeta]\!]\,\mathbb{R}_g(m+2)\ln a)}, \tag{2.2a}$$

$$W_1(r,\mathbb{R}) = -1 + \frac{m\mathbb{K}(\mathbb{R})\,r^2}{m\mathbb{K}(\mathbb{R}) + a^2 - 1 + 2(\mathbb{K}(\mathbb{R})-1)\ln a} \quad (0 \leqslant r \leqslant 1), \tag{2.2b}$$

$$W_2(r,\mathbb{R}) = -\frac{a^2 - r^2 - 2(\mathbb{K}(\mathbb{R})-1)\ln\dfrac{r}{a}}{m\mathbb{K}(\mathbb{R}) + a^2 - 1 + 2(\mathbb{K}(\mathbb{R})-1)\ln a} \quad (1 \leqslant r \leqslant a). \tag{2.2c}$$

In the above formulae, the jump $[\![\cdot]\!]$ is defined as

$$[\![\cdot]\!] = (\cdot)_1 - (\cdot)_2.$$

It is easy to see from these expressions that the up-flow velocity is formally the negative of the down-flow velocity except that the parameter $\mathbb{K}(\mathbb{R})$ is different. However, down-flow and up-flow can be treated uniformly, using the velocity profile (2.1), with $\mathbb{R}_g > 0$ for down-flows and $\mathbb{R}_g < 0$ for up-flows since any up-flow can be obtained from a down-flow by simply reversing the direction of gravity. The basic flow (2.1) depends on the Reynolds number $\mathbb{R}$ through the parameter $\mathbb{K}(\mathbb{R})$.

The perfect core–annular flow (2.1) can be realized if the controlling parameters fall in a certain range. Experiments in a vertical pipe with parameters in this range were described in CBJ. It is also possible to realize the concentric core–annular flow in a horizontal pipe if the densities of oil and water are matched. Experiment 2 of Charles, Govier & Hodgson (1961), called 'oil in water concentric', can be regarded as an example of perfect core–annular flow in a horizontal pipe.

Numerical experiments using linear theory have shown that, without exception, axisymmetric disturbances are most dangerous (see PCJ; HJ; CBJ). Therefore we restrict our analysis to axisymmetric disturbances. Nevertheless, non-axisymmetric waves arise in practice. The photograph of 'corkscrew' waves exhibited in figure 2 is a good example. These 'corkscrew' waves can result from the instabilities due to finite non-axisymmetric disturbances.

For axisymmetric finite disturbances, the disturbance velocity is of the form $\boldsymbol{u} = (u, 0, w)$ in the cylindrical coordinates (r, θ, x) and $\partial(\cdot)/\partial\theta = 0$. The full nonlinear evolution equations for $\boldsymbol{u}$ in dimensionless form are

$$\operatorname{div}\boldsymbol{u} = 0,$$

$$\frac{\partial \boldsymbol{u}}{\partial t} + W\frac{\partial \boldsymbol{u}}{\partial x} + \boldsymbol{e}_x W' + (\boldsymbol{u}\cdot\nabla)\boldsymbol{u} = -\nabla p + \frac{1}{\mathbb{R}_l}\nabla^2\boldsymbol{u}, \tag{2.3}$$

written for axisymmetric flow in cylindrical coordinates, where W is the basic flow and p is the perturbation pressure. These equations hold both in the core, $l = 1$ when $0 \leqslant r \leqslant 1 + \delta(x,t)$, and in the annulus, $l = 2$ when $1 + \delta(x,t) \leqslant r \leqslant a$. $\delta(x,t)$ is the dimensionless deviation of the interface from a perfect cylinder $r = 1$. The primes indicate the derivatives with respect to r. On the pipe wall $r = a$, we have the no-slip condition

$$u = w = 0, \tag{2.4}$$

and at the centre of the pipe, $r = 0$, u, w, p must be bounded.

At the interface, $r = 1 + \delta(x,t)$ we have the kinematic condition

$$u = \frac{\partial\delta}{\partial t} + (W_1 + w_1)\frac{\partial\delta}{\partial x} = \frac{\partial\delta}{\partial t} + (W_2 + w_2)\frac{\partial\delta}{\partial x}, \tag{2.5}$$

and the continuity of velocity

$$[\![u]\!]_\delta = [\![W+w]\!]_\delta = 0, \tag{2.6}$$

where the subscript δ refers to the deformed interface $r = 1+\delta(x,t)$.

The shear stress and normal stress balances on the interface are:

$$[\![m\{(1-\delta_x^2)(W'+u_x+w_r)+2\delta_x(u_r-w_x)\}]\!]_\delta = 0, \tag{2.7}$$

$$-[\![\zeta p]\!]_\delta+\frac{1}{\mathbb{R}_1}\frac{2}{1+\delta_x^2}[\![m\{u_r-\delta_x(W'+u_x+w_r)+\delta_x^2 w_x\}]\!]_\delta = \frac{J^*}{a\mathbb{R}_1^2}\left\{\frac{\delta_{xx}}{(1+\delta_x^2)^{\frac{3}{2}}}-\frac{1}{(1+\delta)(1+\delta_x^2)^{\frac{1}{2}}}+1\right\}, \tag{2.8}$$

where, the subscripts r, x refer to the differentiations with respect to r and x respectively.

To simplify these equations further, we can introduce a perturbation stream function ψ in each region:

$$u = -\frac{\psi_x}{r}, \quad w = \frac{\psi_r}{r}.$$

Then the field equations can be reduced to a single equation for the stream function ψ by eliminating pressure p:

$$(\mathscr{L}\psi)_t-\left(W''-\frac{W'}{r}\right)\psi_x+\left(W+\frac{1}{r}\psi_r\right)\{\mathscr{L}\psi)_x-\frac{1}{r}\psi_x(\mathscr{L}\psi)_r+\frac{2}{r^2}\psi_x\mathscr{L}\psi = \frac{1}{\mathbb{R}_l}\mathscr{L}^2\psi \tag{2.9}$$

where the operator $\mathscr{L}$ is defined as

$$\mathscr{L} = \frac{\partial^2}{\partial r^2}-\frac{1}{r}\frac{\partial}{\partial r}+\frac{\partial^2}{\partial x^2}.$$

$$\text{At } r = a: \quad \psi = \psi_r = 0. \tag{2.10}$$

$$\text{At } r = 0: \quad \psi = \psi_r = 0. \tag{2.11}$$

All the interface conditions can be expressed in terms of the perturbation stream function ψ, resulting in a system of differential equations for $\psi_1(r,x,t)$, $\psi_2(r,x,t)$ and $\delta(x,t)$.

To study weakly nonlinear stability, we expand the interfacial conditions around the unperturbed interface $r = 1$ and truncate the Taylor series at order $O(\delta^3)$. For this purpose we notice that from the linear theory, we have

$$u \sim w \sim \delta. \tag{2.12}$$

The resulting interface conditions up to the third order can be summarized as:

Kinematic condition:

$$\mathscr{L}_{i1}(\psi_l,\delta) = \mathscr{Q}_{i1}(\psi_l,\delta)+\mathscr{C}_{i1}(\psi_l,\delta), \tag{2.13a}$$

Continuity of velocity:

$$[\![\mathscr{L}_{i2}(\psi)]\!] = \mathscr{Q}_{i2}(\psi_1,\psi_2,\delta)+\mathscr{C}_{i2}(\psi_1,\psi_2,\delta), \tag{2.13b}$$

$$[\![\mathscr{L}_{i3}(\psi,\delta)]\!] = \mathscr{Q}_{i3}(\psi_1,\psi_2,\delta)+\mathscr{C}_{i3}(\psi_1,\psi_2,\delta), \tag{2.13c}$$

Shear stress balance:

$$[\![m\mathscr{L}_{i4}(\psi,\delta)]\!] = \mathscr{Q}_{i4}(\psi_1,\psi_2,\delta)+\mathscr{C}_{i4}(\psi_1,\psi_2,\delta), \tag{2.13d}$$

Normal stress balance:

$$[\![\mathscr{L}_{i5}(\psi,\delta)]\!]-\frac{J^*}{a\mathbb{R}_1^2}(\delta_{xxx}+\delta_x)=\mathscr{Q}_{i5}(\psi_1,\psi_2,\delta)+\mathscr{C}_{i5}(\psi_1,\psi_2,\delta). \tag{2.13e}$$

In the above expressions, the jump $[\![(\cdot)]\!]$ without subscript δ refers to the jump evaluated at the undeformed interface $r=1$ and all the quantities are evaluated at $r=1$ as well. The symbols $\mathscr{L}$, $\mathscr{Q}$, $\mathscr{C}$ refer to linear, quadratic and cubic differential operators respectively. The subscripts i indicate that all these operators are defined on the interface $r=1$ only. These interfacial operators are listed in the Appendix to this paper. The reduced system (2.9), (2.10), (2.11) and (2.13) is used to derive the amplitude equation.

3. Multiple scales, wave packets and Ginzburg–Landau equation

The derivation of the amplitude equation near criticality using the techniques of multiple scales is now well known and the details can be found in Newell (1974) or Stewartson & Stuart (1971). We introduce a small perturbation parameter ϵ, defined by

$$\epsilon^2=|d_{1r}(\mathbb{R}-\mathbb{R}_c)| \tag{3.1}$$

where we have adopted the notation of Stewartson & Stuart (1971) for d_{1r}

$$d_{1r}=\mathrm{Re}\{d_1\},\quad d_1=-\mathrm{i}\left\{\frac{\partial(\alpha c)}{\partial\mathbb{R}}\right\}_{(\alpha_c,\,\mathbb{R}_c)}. \tag{3.2}$$

Here $-\mathrm{i}\alpha c$ is the linear complex growth rate for the linear instability of the basic flow and $(\alpha_c,\mathbb{R}_c)$ is the point at the nose of the neutral curve. This critical point is a minimum on the upper branch of the neutral curve and a maximum on the lower branch. Here, 'upper' and 'lower' refer to the bifurcation parameter $\mathbb{R}$, not the wavenumber α as traditionally assigned. The basic flow loses stability as $\mathbb{R}$ is increased past $\mathbb{R}_c$ on the upper branch. Here, $d_{1r}>0$ on the upper branch, and $d_{1r}<0$ on the lower branch. We may consider the first case $d_{1r}>0$, $\mathbb{R}>\mathbb{R}_c$ and then generalize to cover all the possibilities.

Introduce the slow spatial and timescales

$$\xi=\epsilon(x-c_g t),\quad \tau=\epsilon^2 t, \tag{3.3a}$$

where c_g is the group velocity at criticality. These scales are appropriate for a wave packet centred at the nose of the neutral curve and the long-time behaviour of this wavetrain is examined in the frame moving with its group velocity c_g. The perturbation stream function ψ and the interface deviation δ are assumed to be slowly varying functions of ξ,τ:

$$\left.\begin{aligned}&\psi\to\psi(\xi,\tau;r,x,t),\\&\delta\to\delta(\xi,\tau;x,t),\\&\frac{\partial}{\partial t}\to\frac{\partial}{\partial t}-\epsilon c_g\frac{\partial}{\partial\xi}+\epsilon^2\frac{\partial}{\partial\tau},\\&\frac{\partial}{\partial x}\to\frac{\partial}{\partial x}+\epsilon\frac{\partial}{\partial\xi}.\end{aligned}\right\} \tag{3.3b}$$

We then define the travelling wave factor of the amplitude

$$E\overset{\text{def.}}{=}\exp[\mathrm{i}\alpha_c(x-c_r t)], \tag{3.4}$$

where c_r is the phase speed at criticality. For a wave packet centred around the critical state, we can assume that ψ and δ have the following form:

$$\left.\begin{aligned}\psi &= \psi_0(r,\xi,\tau)+\{\psi_1(r,\xi,\tau)E+\text{c.c.}\}+\{\psi_2(r,\xi,\tau)E^2+\text{c.c.}\}+\text{h.h.}\\ \delta &= \delta_0(\xi,\tau)+\{\delta_1(\xi,\tau)E+\text{c.c.}\}+\{\delta_2(\xi,\tau)E^2+\text{c.c.}\}+\text{h.h.},\end{aligned}\right\} \tag{3.5}$$

where c.c. stands for complex conjugate and h.h. for higher harmonics. We assume that the fundamental wave $\psi_1(r,\xi,\tau)E$ is of order ϵ and expansions in ϵ yield

$$\left.\begin{aligned}\psi_1 &= \epsilon\psi_{11}(r,\xi,\tau)+\epsilon^2\psi_{12}(r,\xi,\tau)+\epsilon^3\psi_{13}(r,\xi,\tau)+O(\epsilon^4),\\ \psi_2 &= \epsilon^2\psi_{22}(r,\xi,\tau)+O(\epsilon^4),\\ \psi_0 &= \epsilon^2\psi_{02}(r,\xi,\tau)+O(\epsilon^4),\end{aligned}\right\} \tag{3.6}$$

and similarly,

$$\left.\begin{aligned}\delta_1 &= \epsilon\delta_{11}(\xi,\tau)+\epsilon^2\delta_{12}(\xi,\tau)+\epsilon^3\delta_{13}(\xi,\tau)+O(\epsilon^4),\\ \delta_2 &= \epsilon^2\delta_{22}(\xi,\tau)+O(\epsilon^4),\\ \delta_0 &= \epsilon^2\delta_{02}(\xi,\tau)+O(\epsilon^4).\end{aligned}\right\} \tag{3.7}$$

Substituting the above expansions into the nonlinear systems of equations and identifying different orders $(k,n)\Leftrightarrow(E^k,\epsilon^n)$ results in a sequence of differential equations. To obtain the amplitude equation at lowest order, we only need to consider the $k=0,1,2$ exponentials (3.4) and the $n=1,2,3$ powers of the small parameter ϵ.

At order $(1,1)$ we have the linear eigenvalue problem at criticality and, if we denote the eigenfunction at criticality to be $\varphi(r)$, then

$$\begin{aligned}\psi_{11}(r,\xi,\tau) &= A(\xi,\tau)\varphi(r),\\ \delta_{11}(\xi,\tau) &= A(\xi,\tau)\eta_{11},\end{aligned} \tag{3.8}$$

where η_{11} is a constant which can be expressed in terms of the value of φ at $r=1$ and $A(\xi,\tau)$ is the slowly varying amplitude of the fundamental wave. The equations which arise at orders $(0,2)$, $(2,2)$, $(1,2)$ support separated product solutions of the following type

$$\left.\begin{aligned}\psi_{02}(r,\xi,\tau) &= |A(\xi,\tau)|^2F(r),\\ \delta_{02}(\xi,\tau) &= |A(\xi,\tau)|^2\eta_{02};\\ \psi_{22}(r,\xi,\tau) &= A^2(\xi,\tau)G(r),\\ \delta_{22}(\xi,\tau) &= A^2(\xi,\tau)\eta_{22};\\ \psi_{12}(r,\xi,\tau) &= \frac{\partial A(\xi,\tau)}{\partial\xi}H(r)+A_2(\xi,\tau)\varphi(r),\\ \delta_{12}(\xi,\tau) &= \frac{\partial A(\xi,\tau)}{\partial\xi}\eta_{12}+A_2(\xi,\tau)\eta_{11}.\end{aligned}\right\} \tag{3.9}$$

Then at orders $(1,2)$ and $(1,3)$, we have

$$\begin{aligned}\mathscr{L}_1(H,\eta_{12}) &= \mathscr{F}(\varphi(r),c_g),\\ \mathscr{L}_1(\psi_{13},\delta_{13}) &= J_1\frac{\partial A}{\partial\tau}+J_2\frac{\partial^2A}{\partial\xi^2}+J_3A+J_4|A|^2A+J_5\frac{\partial A_2}{\partial\xi},\end{aligned} \tag{3.10}$$

where $\mathscr{L}_1$ is the linear Orr–Sommerfeld operator at criticality and $J_i, i=\ldots,5$ are functions of $\varphi(r)$, $F(r)$, $G(r)$ and $H(r)$. Applying the Fredholm alternative at order

(1, 2), we can obtain a formula determining the group velocity c_g. At order (1, 3), the application of the Fredholm alternative yields the Ginzburg–Landau equation governing the amplitude $A(\xi, \tau)$ of the fundamental wave,

$$\frac{\partial A}{\partial \tau} - a_2 \frac{\partial^2 A}{\partial \xi^2} = \frac{d_1}{d_{1r}} A - l|A|^2 A. \tag{3.11}$$

The term $\partial A_2/\partial \xi$ does not appear because its coefficient vanishes when the group velocity c_g is properly expressed using the Fredholm alternative. The complementary part of the solution of the singular problem at order (1, 2) has no effect on the final amplitude equation. The coefficient of the cubic term, l, is called the first Landau constant and it depends on all the lower-order solutions. The coefficients a_2, d_1 and l are complex in general and can be computed using the Fredholm alternative. For non-degenerate cases, the real part of a_2 is always positive for both the upper and the lower branch because the growth rate reaches a maximum at the critical point, the nose of the neutral curve ($a_{2r} = 0$ if the neutral curve has a higher-order (> 2) contact with $\mathbb{R} = \mathbb{R}_c$).

We may write the Ginzburg–Landau equation in a uniform form, valid for both the upper and lower branch of the neutral curves,

$$\frac{\partial A}{\partial \tau} - a_2 \frac{\partial^2 A}{\partial \xi^2} = \operatorname{sgn}(d_{1r}) \operatorname{sgn}(\mathbb{R} - \mathbb{R}_c) \frac{d_1}{d_{1r}} A - l|A|^2 A, \tag{3.12}$$

by taking proper account of the various sign possibilities offered by (3.1). The parameter $\operatorname{sgn}(d_{1r}) \operatorname{sgn}(\mathbb{R} - \mathbb{R}_c)$ measures the distance from the bifurcation threshold (linear growth or damping), $\operatorname{sgn}(d_{1r}) \operatorname{sgn}(\mathbb{R} - \mathbb{R}_c)(d_{1i}/d_{1r})$ corresponds to the frequency shift due to the linear dispersion; a_{2r}, a_{2i}, l_r, l_i are associated with diffusion ($a_{2r} > 0$), dispersion, nonlinear saturation ($l_r > 0$) and nonlinear renormalization of the frequency, respectively (the subscripts r, i refer to the real and imaginary parts of a coefficient).

The Landau constant l depends on the normalization of the eigenvector $\varphi(r)$ of the spectral problem but is independent of the normalization of the adjoint eigenvector. If we use a different normalization for the eigenvector $\varphi(r)$ such that

$$\varphi(r) \to q\varphi(r), A(\xi, \tau) \to qA(\xi, \tau),$$

where q is any non-zero constant, we find, using (3.12), that

$$\frac{\partial A}{\partial \tau} - a_2 \frac{\partial^2 A}{\partial \xi^2} = \operatorname{sgn}(d_{1r}) \operatorname{sgn}(\mathbb{R} - \mathbb{R}_c) \frac{d_1}{d_{1r}} A - l|q|^2 |A|^2 A. \tag{3.13}$$

The Landau constant will become unique if a well-defined amplitude is introduced. This is especially important when pursuing higher-order Landau constants (Joseph & Sattinger 1972; Herbert 1980; Sen & Venkateswarlu 1983). In the lowest-order case, the Ginzburg–Landau equation (3.12), we can simply rescale the amplitude function $A(\xi, \tau)$

$$A(\xi, \tau) \to \frac{A(\xi, \tau)}{|q|(|l_r|)^{\frac{1}{2}}} \tag{3.14}$$

where $l = l_r + il_i$, to get a Ginzburg–Landau equation with coefficients independent of q:

$$\frac{\partial A}{\partial \tau} - a_2 \frac{\partial^2 A}{\partial \xi^2} = \operatorname{sgn}(d_{1r}) \operatorname{sgn}(\mathbb{R} - \mathbb{R}_c) \frac{d_1}{d_{1r}} A - (\operatorname{sgn}(l_r) + iC_n)|A|^2 A, \tag{3.15}$$

where $C_n = l_i/|l_r|$ is a parameter independent of the normalization condition for $\varphi(r)$.

Another useful rescaled form of (3.13) can be obtained by introducing the following transformations:

$$A(\xi,\tau) = \frac{\hat{A}(\xi,\tau)}{|q|\,(|l_r|)^{\frac{1}{2}}}\exp\left[\mathrm{i}\,\mathrm{sgn}\,(d_{1r})\,\mathrm{sgn}\,(\mathbb{R}-\mathbb{R}_c)\frac{d_{1i}}{d_{1r}}\right],$$

$$\hat{\xi} = \frac{\xi}{(|a_{2r}|)^{\frac{1}{2}}}, \quad C_d = \frac{a_{2i}}{|a_{2r}|}, \quad C_n = \frac{l_i}{|l_r|}. \tag{3.16}$$

After dropping the carets, we get

$$\frac{\partial A}{\partial \tau} - (\mathrm{sgn}\,(a_{2r}) + \mathrm{i}C_d)\frac{\partial^2 A}{\partial \xi^2} = \mathrm{sgn}\,(d_{1r})\,\mathrm{sgn}\,(\mathbb{R}-\mathbb{R}_c)\,A - (\mathrm{sgn}\,(l_r + \mathrm{i}C_n)\,|A|^2 A. \tag{3.17}$$

The form (3.17) was first introduced by Moon, Huerre & Redekopp (1983) in their study of transition to chaos in solutions of the Ginzburg–Landau equation. Since $a_{2r} > 0$ we can replace $\mathrm{sgn}\,(a_{2r})$ by $+1$.

Equation (3.17) can be regarded as the canonical form of the Ginzburg–Landau equation. It admits a travelling wave solution of the form

$$A(\xi,\tau) = A_0 \exp\left[\mathrm{i}(\beta_0\,\xi - \gamma_0\,\tau)\right]$$

where A_0, β_0, γ_0 are all real constants defined in terms of the coefficients of (3.17). The stability of the travelling-wave solution was studied by Newell (1974), Stuart & DiPrima (1978) and Moon (1982). Their analyses provide a unified treatment of the well-known Eckhaus instability and the Benjamin–Feir instability, and their results are also framed in terms of the coefficients of (3.17). When the real part of the Landau constant, l_r, is positive, there are soliton-like solutions which have been discussed by Hocking & Stewartson (1972). These solutions have been called 'breather' by Holmes (1986).

The spectral problem (1, 1) and the boundary-value problems at orders (0, 2), (2, 2), and (1, 2) which are needed to compute the coefficients obf the Ginzburg–Landau equation (3.12) are listed in Chen (1990). We note that at each order the interface parameter η can be eliminated. All the algebraic operations are carried out by the symbolic manipulator REDUCE2 and independently checked by hand. An efficient method to compute the coefficients of the Ginzburg–Landau equation is presented in the next section. Interested readers may apply the theory of modulated plane wave and soliton-like structures to the problem of water-lubricated pipelining using these coefficients. We see large-amplitude (bamboo) waves in our experiments, but they have average wavelengths of the same order as the monochromatic waves. We have concluded that our large waves are not modulated monochromatic waves and that they seem not to be described by Ginzburg–Landau equations.

4. Singular value decomposition and its application to the numerical computation of the coefficients of amplitude equations and normal forms

There are many universal equations used as model equations for the study of physical processes. These equations arise as an asymptotic solvability condition, which is a condition on the leading-order approximation to the solution of a more

complicated set of equations which ensures that the later iterates of the approximation remain uniformly bounded. Examples of these equations are the Korteweg–de Vries equation and its generalizations, the Ginzburg–Landau equation and its generalizations and the Davey–Stewartson equations (Craik 1983; Newell 1985). For parallel shear flows, the coefficients of these model equations are in general given by very lengthy domain integrals expressing solvability conditions, commonly known as the Fredholm alternative.

The Fredholm alternative requires that the inhomogeneous terms in the underlying system of differential equations, which contain the unknown coefficients, be orthogonal to the independent eigenvector spanning the null space of the adjoint system of differential equations. Typically the underlying system of the inhomogeneous differential equation is discretized and solved as an inhomogeneous matrix-valued problem. We find that the solvability conditions which lead to values of the unknown coefficients are conveniently and economically computed by application of the singular value decomposition directly to the matrix formulation.

The singular value decomposition (SVD) is one of the most important decompositions in matrix algebra and is widely used for statistics and for solving least-squares problems (see Golub & Van Loan 1983). The decomposition theorem can be stated as follows: each and every $M \times N$ complex valued matrix $\boldsymbol{T}$ can be reduced to diagonal form by unitary transformations $\boldsymbol{U}$ and $\boldsymbol{V}$,

$$\boldsymbol{T} = \boldsymbol{U}\,\mathrm{diag}\,[\sigma_1, \sigma_2, \ldots, \sigma_N]\,\boldsymbol{V}^{\mathrm{H}}, \tag{4.1}$$

where $\sigma_1 \geqslant \sigma_2 \geqslant ,,, \geqslant \sigma_N \geqslant 0$ are real-valued scalars, called the singular values of $\boldsymbol{T}$. Here $\boldsymbol{U}$ is an $M \times N$ column orthonormal matrix, $\boldsymbol{V}$ an $N \times N$ unitary matrix and $\boldsymbol{V}^{\mathrm{H}}$ is the Hermitian transpose of $\boldsymbol{V}$. The columns of $\boldsymbol{U}$ and $\boldsymbol{V}$ are called the left and right singular vectors of $\boldsymbol{T}$ respectively.

When $M = N$, $\boldsymbol{T}$ is a square matrix and

$$\boldsymbol{U}\boldsymbol{U}^{\mathrm{H}} = \boldsymbol{U}^{\mathrm{H}}\boldsymbol{U} = \boldsymbol{I}, \tag{4.2}$$

$$\boldsymbol{V}\boldsymbol{V}^{\mathrm{H}} = \boldsymbol{V}^{\mathrm{H}}\boldsymbol{V} = \boldsymbol{I}. \tag{4.3}$$

Consider the generalized matrix eigenvalue problem

$$(\boldsymbol{A} - c\boldsymbol{B})\,\boldsymbol{x} = 0, \tag{4.4}$$

where $\boldsymbol{A}, \boldsymbol{B}$ are both square $N \times N$ complex matrices. Assume that c is an semi-simple eigenvalue of (4.4) with algebraic and geometric multiplicity K. Then applying SVD to the matrix $\boldsymbol{A} - c\boldsymbol{B}$, we get

$$\boldsymbol{A} - c\boldsymbol{B} = \boldsymbol{U}\,\mathrm{diag}\,[\sigma_1, \sigma_2, \ldots, \sigma_{N-K}, 0, 0, \ldots, 0]\,\boldsymbol{V}^{\mathrm{H}}, \tag{4.5}$$

where $\sigma_1 \geqslant \sigma_2 \geqslant \ldots \geqslant \sigma_{N-K} > 0$ are real constants. Let

$$\boldsymbol{U} = [\boldsymbol{u}_1, \boldsymbol{u}_2, \ldots, \boldsymbol{u}_{N-K}, \boldsymbol{u}_{N-K+1}, \ldots, \boldsymbol{u}_N], \tag{4.6}$$

$$\boldsymbol{V} = [\boldsymbol{v}_1, \boldsymbol{v}_2, \ldots, \boldsymbol{v}_{N-K}, \boldsymbol{v}_{N-K+1}, \ldots, \boldsymbol{v}_N], \tag{4.7}$$

where $\boldsymbol{u}_j, \boldsymbol{v}_j (j = 1, \ldots, N)$ are the column vectors of matrices, $\boldsymbol{U}$ and $\boldsymbol{V}$ respectively. From (4.4) and (4.5) we see that $\mathrm{diag}\,[\sigma_1, \sigma_2, \ldots, \sigma_{N-K}, 0, 0, \ldots, 0]\,\boldsymbol{y} = 0$, where $\boldsymbol{V}^{\mathrm{H}}\boldsymbol{x} = \boldsymbol{y}$ and $\boldsymbol{x}$ is the eigenvector corresponding to the eigenvalue c. Therefore we have

$$\boldsymbol{V}^{\mathrm{H}}\boldsymbol{x} = \boldsymbol{y} = [0, 0, \ldots, 0, y_{N-K+1}, \ldots, y_N], \tag{4.8}$$

where $y_{N-K+1}, \ldots, y_N$ are K arbitrary constants. Then $\boldsymbol{x} = \boldsymbol{V}\boldsymbol{y}$ is an eigenvector of

$\boldsymbol{A}-c\boldsymbol{B}$. We find, in this way, that the column vectors $\boldsymbol{v}_j, j = N-K+1, \ldots, N$, are the K independent eigenvectors corresponding to c, normalized with

$$\boldsymbol{v}_j^* \boldsymbol{v}_j^{\mathrm{T}} = 1 \quad (j = N-K+1, \ldots, N),$$

where star * denotes the complex conjugate and superscript T for transpose. Similarly the column vectors $\boldsymbol{u}_j, j = N-K+1, \ldots, N$, are the K independent eigenvectors of the problem adjoint to (4.4):

$$(\boldsymbol{A}-c\boldsymbol{B})^{\mathrm{H}} \boldsymbol{x} = 0. \tag{4.9}$$

They are the corresponding adjoint eigenvectors, normalized with

$$\boldsymbol{u}_j^* \boldsymbol{u}_j^{\mathrm{T}} = 1 \quad (j = N-K+1, \ldots, N).$$

The application of SVD to solve the inhomogeneous system of algebraic equations

$$(\boldsymbol{A}-c\boldsymbol{B})\boldsymbol{x} = \boldsymbol{f} \tag{4.10}$$

is straightforward. Suppose c is an semi-simple eigenvalue of (4.4) of multiplicity K. We use SVD to decompose $\boldsymbol{A}-c\boldsymbol{B}$ in the form (4.5). We then compute

$$\mathrm{diag}\,[\sigma_1, \sigma_2, \ldots, \sigma_{N-K}, 0, 0, \ldots, 0]\, \boldsymbol{V}^{\mathrm{H}} \boldsymbol{x} = \boldsymbol{U}^{\mathrm{H}} \boldsymbol{f}. \tag{4.11}$$

The last K components of the vector on the left of (4.11) are identically zero and so must be those on the right. This defines the Fredholm alternative, i.e. the solvability conditions

$$\boldsymbol{u}_j^* \boldsymbol{f}^{\mathrm{T}} = 0 \quad (j = N-K+1, \ldots, N), \tag{4.12}$$

for the inhomogeneous matrix problem (4.10). The conditions (4.12) are necessary and sufficient for solvability of the inhomogeneous problem (4.10) in $\boldsymbol{C}$ when c is an eigenvalue of $\boldsymbol{A}$ relative to $\boldsymbol{B}$.

The solution to the inhomogeneous equation (4.10) is given by

$$\boldsymbol{x} = \boldsymbol{V}_s \boldsymbol{g} + \sum_{j=N-K+1}^{N} \beta_j \boldsymbol{v}_j, \tag{4.13}$$

where the $N \times (N-K)$ matrix $\boldsymbol{V}_s$ is given by

$$\boldsymbol{V}_s = [\boldsymbol{v}_1, \boldsymbol{v}_2, \ldots, \boldsymbol{v}_{N-K}],$$

with $\boldsymbol{v}_{1,2}, \ldots, \boldsymbol{v}_{N-K}$ given by (4.7) and the vector $\boldsymbol{g}$ has $N-K$ components given by

$$\boldsymbol{g} = [\sigma_1^{-1} \boldsymbol{u}_1^* \boldsymbol{f}^{\mathrm{T}}, \sigma_2^{-1} \boldsymbol{u}_2^* \boldsymbol{f}^{\mathrm{T}}, \ldots, \sigma_{N-K}^{-1} \boldsymbol{u}_{N-K}^* \boldsymbol{f}^{\mathrm{T}}],$$

where the $\boldsymbol{u}_j$ are those given by (4.6). The β_j are constants and can be determined by K normalization conditions.

Applications of the above SVD algorithm to bifurcation theory have been presented by Chen & Joseph (1990). Independently, Newell, Passot & Souli (1989) applied the same algorithm to the bifurcation study of convection at finite Rayleigh numbers in large containers. The algorithm takes advantage of the matrix formulations of the perturbation problems stated in §3. Specifically, the problems $(0, 2)$, $(2, 2)$ are invertible and $(1, 2)$, $(1, 3)$ are singular. For these singular problems, a singular system of algebraic equations of the form (4.10) arises after discretization and the technique described above is readily applicable. For the spectral problem, we have

$$(\boldsymbol{A}-c_{\mathrm{r}}\boldsymbol{B})\boldsymbol{\varphi} = 0,$$

where the matrix $\boldsymbol{A}-c_{\mathrm{r}}\boldsymbol{B}$ and the vector $\boldsymbol{\varphi}$ result from the discretization of the

	RP, DHS	Present
c_g	0.383	0.3831
d_1	$(0.168+\mathrm{i}0.811)\times10^{-5}$	$(0.1683+\mathrm{i}0.8113)\times10^{-5}$
a_2	$0.187+\mathrm{i}0.0275$	$0.1867+\mathrm{i}0.0275$
l	$-30.3+\mathrm{i}173$	$-30.94+\mathrm{i}172.83$

TABLE 1. Comparison of the coefficients of Ginzburg–Landau equation for one fluid plane Poiseuille flow, $\alpha_c = 1.02$, $\mathbb{R}_c = 5772.22$

Orr–Sommerfeld operator at criticality and the eigenfunction $\varphi(r)$, respectively. At orders (1, 2) and (1, 3), we have the following singular algebraic equations

$$(\boldsymbol{A}-c_r\boldsymbol{B})\,\boldsymbol{h} = \boldsymbol{f}(\varphi, c_g) \tag{4.14}$$

$$(\boldsymbol{A}-c_r)\,\boldsymbol{B}_{13} = \frac{\partial A}{\partial \tau}\boldsymbol{f}_1 + \frac{\partial^2 A}{\partial \xi^2}\boldsymbol{f}_2 + \frac{A}{d_{1r}}\boldsymbol{f}_3 + |A|^2 A\boldsymbol{f}_4. \tag{4.15}$$

Assume at criticality c_r is semi-simple with multiplicity $K = 1$. Then (4.14) can be solved by first using the solvability condition (4.12) to evaluate the group velocity c_g and then using the formula (4.13) without the complementary part ($\beta_j = 0$) because of the fact that the complementary part has no contribution to the final amplitude equation. Application of the solvability condition (4.12) to (4.15) generates the coefficients of the Ginzburg–Landau equation (3.12):

$$a_2 = -\boldsymbol{u}_N^* \boldsymbol{f}_2^{\mathrm{T}} / \boldsymbol{u}_N^* \boldsymbol{f}_1^{\mathrm{T}},$$
$$d_1 = -\boldsymbol{u}_N^* \boldsymbol{f}_3^{\mathrm{T}} / \boldsymbol{u}_N^* \boldsymbol{f}_1^{\mathrm{T}},$$
$$l = \boldsymbol{u}_N^* \boldsymbol{f}_4^{\mathrm{T}} / \boldsymbol{u}_N^* \boldsymbol{f}_1^{\mathrm{T}},$$

and

$$\boldsymbol{u}_N^* \boldsymbol{f}_1^{\mathrm{T}} \neq 0.$$

The above procedure was applied to the problem of one-fluid plane Poiseuille flow and the computed values were compared with values obtained by Reynolds & Potter (1967) (RP) and Davey, Hocking & Stewartson (1974) (DHS) using analytical formulae. In order to compare the accuracy of the present scheme, the same normalization condition for the eigenvector as in RP and DHS is used to make the Landau constant unique. The results are presented in table 1. It can be seen that the present algorithm gives accurate and reliable results and should find a wide range of applications in similar situations. The same algorithm is applied to the bifurcation analysis of core–annular flows and a Chebychev pseudo-spectral method is used for the discretizations of the differential equations.

For all the calculations we performed for nonlinear stability of core–annular flows, we normalize the eigen-streamfunctions φ_1 and φ_2 with discrete L_2 norms such that $\|\varphi_1\|^2 + \|\varphi_2\|^2 = 1$. Most of our results are summarized in tables 2–8.

5. Nonlinear stability of core–annular flows

The nature of the bifurcation of core–annular flows is determined by the real part of the Landau constants l in (3.12). If $l_r > 0$, the bifurcation is supercritical and a finite-amplitude equilibrium solution exists. On the other hand, if $l_r < 0$, the bifurcation is subcritical; the bifurcating solution of (3.12) will burst in finite time and a higher-order theory is needed (Hocking, Stewartson & Stuart 1972).

The coefficients of Ginzburg–Landau equations for different parameters are listed in tables 2–7. Since we are mainly interested in the direction of the bifurcations, we

(*a*) Upper branch of the neutral curve

m	α_c	$\mathbb{R}_c$	C_d	sgn (l_r)	C_n
0.9	2.99	175.033	5.0054	+	−11.4151
0.85	3.2	162.23	5.0375	+	−197.3133
0.8	3.3	150.71	4.9972	−	−6.7538
0.7	3.6	128.72	4.3832	−	−1.2640
0.5	9.1	55.61	−0.7895	−	−1.3827
0.2	5.8	16.24	−1.0769	−	−0.8101
0.1	4.4	9.985	−0.4983	−	0.1714

(*b*) Lower branch of the neutral curve

0.9	0.09	5.6047	7.0	+	−5.6021
0.85	0.06	4.7010	4.3030	+	−3.9426
0.8	0.04	4.0821	6.7899	+	−5.5512
0.7	0.03	3.3751	42.8759	+	−31.0698
0.5	0.05	2.78	23.3539	−	20.4787
0.2	0.029	2.6341	245.4459	−	254.3165
0.1	0.06	2.707	71.4207	−	72.8215

TABLE 2. Coefficients of GL equations for $a = 1.25$, $\zeta_2 = 1$, $J^* = 1$, down-flow

(*a*) Upper branch of the neutral curve

ζ_2	α_c	$\mathbb{R}_c$	C_d	sgn (l_r)	C_n
1.0	3.6	128.72	4.3832	−	−1.2640
1.2	1.95	1592.3	4.1387	+	0.1952
1.4	2.7	1060.74	1.2524	+	−0.1585
1.6	3.28	791.31	1.0583	+	−0.2605

(*b*) Lower branch of the neutral curve

1.0	0.03	3.3751	42.8759	+	−31.0698
1.2	0.04	3.1830	35.5138	+	−19.6098
1.4	0.01	3.071	1.5466	+	−1.6507
1.6	0.01	2.93	1.4688	+	−1.4710

TABLE 3. Coefficients of GL equations for $a = 1.25$, $m = 0.7$, $J^* = 1$, $\mathbb{R}_g = 0.5$, down-flow

(*a*) Upper branch of the neutral curve

ζ_2	α_c	$\mathbb{R}_c$	C_d	sgn (l_r)	C_n
1.0	9.1	55.61	−0.7895	−	−1.3827
1.2	1.9	543.6	11.2156	+	0.7736
1.4	2.71	568.68	1.6348	+	−0.1513
1.6	3.1	469.25	1.4034	+	−0.4332

(*b*) Lower branch of the neutral curve

1.0	0.05	2.78	23.3539	−	20.4787
1.2	0.08	2.523	14.9791	−	13.8764
1.4	0.04	2.3228	61.18	−	51.4451
1.6	0.08	2.1801	9.2344	−	8.4382

TABLE 4. Coefficients of GL equations for $a = 1.25$, $m = 0.5$, $J^* = 1$, $\mathbb{R}_g = 0.5$, down-flow

(*a*) Upper branch of the neutral curve

ζ_2	α_c	$\mathbb{R}_c$	C_d	sgn (l_r)	C_n
0.5	7.26	140.871	5.7827	−	−2.4054
0.8	8.91	235.084	4.7197	−	−0.8352
1.0	24.77	156.451	1.1180	−	5.2623
1.2	24.36	136.034	1.1141	−	12.0131
1.4	24.05	121.916	1.0833	−	273.0102
1.5	23.92	116.355	1.0514	+	44.9198
1.6	23.82	111.522	1.0179	+	24.6314

(*b*) Lower branch of the neutral curve

0.5	0.1	1.08	−11.9596	−	−7.2965
0.8	0.15	1.051	−9.3205	−	−6.5107
1.0	0.05	1.044	−58.0376	−	−28.6788
1.2	0.09	1.034	−15.1812	−	−10.8792
1.4	0.14	1.0202	−9.5561	−	−7.2649
1.5	0.06	1.019	−21.2016	−	−0.8362
1.6	0.1	1.0	−23.6511	−	−14.7862

TABLE 5. Coefficients of GL equations for $a = 1.1$, $m = 0.5$, $J^* = 1$, $\mathbb{R}_g = 0.5$, down-flow

(*a*) Upper branch of the neutral curve

ζ_2	α_c	$\mathbb{R}_c$	C_d	sgn (l_r)	C_n
0.5	2.03	619.53	−0.2407	+	−1.7274
0.6	2.16	706.80	−0.1143	+	−2.6185
0.7	2.31	824.45	0.0196	+	−6.3772
0.8	2.53	994.30	0.1235	−	−5.0004
1.0	3.56	1490.16	0.3926	−	−0.3405
1.2	7.67	2025.59	−0.2422	−	−6.9622
1.4	8.80	1700.47	−0.4030	−	−2.6566
1.5	9.55	1537.17	−0.5902	−	−34.1854
1.6	10.36	1390.44	−0.8053	+	0.8573
1.8	11.91	1162.06	−1.1776	+	1.9673

(*b*) Lower branch of the neutral curve

0.5	0.26	47.91	−5.9844	−	−0.7709
0.6	0.24	47.70	−7.0583	−	−0.8770
0.7	0.22	47.50	−8.2410	−	−0.9921
0.8	0.22	47.30	−7.7273	−	−0.9799
1.0	0.20	46.92	−8.3867	−	−1.0912
1.2	0.16	46.464	−11.6444	−	−1.4088
1.4	0.1	46.22	−21.4375	−	−2.2710
1.5	0.11	46.053	−16.9091	−	−2.0493
1.6	0.11	45.89	−16.0870	−	−2.0335
1.8	0.09	45.56	−18.9375	−	−2.4719

TABLE 6. Coefficients of GL equations for $a = 1.1$, $m = 0.5$, $J^* = 2000$, $\mathbb{R}_g = 0.5$, down-flow

have only listed the values of the critical states $(\alpha_c, \mathbb{R}_c(\alpha_c))$, sgn (l_r), C_d and C_n in these tables, corresponding to the canonical form (3.17). The values of c_r, c_g, d_1, a_2 and l are documented in Chen (1990). The first thing to look at in these tables is the next to the last column labelled sgn (l_r). A plus sign here means that the bifurcation is supercritical, a minus sign that it is subcritical.

The cases studied in tables 2–7 explore the general features of bifurcation of

ζ_2	α_c	$\mathbb{R}_c$	C_d	sgn (l_r)	C_n
		(*a*) Upper branch of the neutral curve			
0.5	1.55	1347.87	−0.7492	+	1.0261
1.0	2.63	2701.37	−0.3912	+	0.1679
1.2	4.18	7126.05	0.0020	−	104.0321
1.5	3.87	6503.75	0.6476	−	−0.3164
2.0	6.81	3202.31	0.1169	−	−1.9525
3.0	13.46	1381.32	−1.3575	−	−5.8459
4.5	15.50	990.06	−1.1833	+	0.2410
		(*b*) Lower branch of the neutral curve			
0.5	0.52	150.26	−0.7910	+	0.5327
1.0	0.51	145.26	−0.7624	+	0.5031
1.2	0.503	143.47	−0.7740	+	0.5048
1.5	0.50	140.95	−0.7473	+	0.4812
2.0	0.49	137.17	−0.7418	+	0.4657
3.0	0.47	130.79	−0.7500	+	0.4516
4.5	0.45	123.25	−0.7345	+	0.4175

TABLE 7. Coefficients of GL equations for $a = 1.1$, $m = 0.9$, $J^* = 2000$, $\mathbb{R}_g = 0.5$, down-flow

core–annular flow. The cases with parameters corresponding to some of the experiments of Charles *et al.* (1961) and BCJ are discussed in §8. As mentioned earlier, our bifurcation analysis is only valid near the nose of the neutral curves. This means that such analysis is applicable when the upper and lower branches of the neutral curve are separated, i.e. there exists an interval of Reynolds numbers within which core–annular flow is linearly stable, as in figures 3 and 4. In other words, we can only study those cases where linearly stable core–annular flow is possible. Figure 5 shows the disposition of subcritical and supercritical solutions in the presence of upper and lower branches of neutral curves. PCJ, BCJ have shown that only when the parameters a, m, ζ, J^* fall in a certain subspace of the parameter space is such stable core–annular flow possible. Typically, there is a 'thin lubricating layer effect': small values of $a-1 = R_2/R_1-1$ stabilize core–annular flow. It is also shown by Hu *et al.* (1990), that if the oil is too viscous, $m = \mu_2/\mu_1 \ll 1$, stable core–annular flow cannot be achieved. We have thus restricted our studies in tables 2–7 to those values of a and m, typically small values of $a-1$ and values of m of order 10^{-1}, with which linearly stable core–annular flows are possible.

The parameter $|\mathbb{R}_g| = 0.5$ is used for all the cases considered in tables 2–7. This parameter enters into the equations only as a product $(\zeta_2-1)\,\mathbb{R}_g$, and hence plays no role when the densities of the two fluids are the same, $\zeta_2 = 1$. We can vary the effect of effective gravity $(\zeta_2-1)\,\mathbb{R}_g$ by varying the value of ζ_2 for a fixed value of $\mathbb{R}_g$.

We are going to divide the tables into two groups according to the value of capillary number J^*. The first group is for $J^* = 1$, corresponding to weak capillary effects typical for our experiments. The results for $J^* = 1$ are summarized in tables 2–5. The second group is for $J^* = 2000$, corresponding to strong capillary effects. This case is of interest for low-viscosity cores for which the capillary number is large. There is an important difference in the lower branch of the neutral curves when $J^* = 1$ and $J^* = 2000$ that is evident from a comparison of figures 3 and 4. When $J^* = 1$, the maximum value of $\mathbb{R}(\alpha)$ on the lower branch of the neutral curve occurs near $\alpha = 0$. When $J^* = 2000$, the maximum value of $\mathbb{R}(\alpha)$ on the lower branch of the neutral curve occurs at a finite value near 0.6.

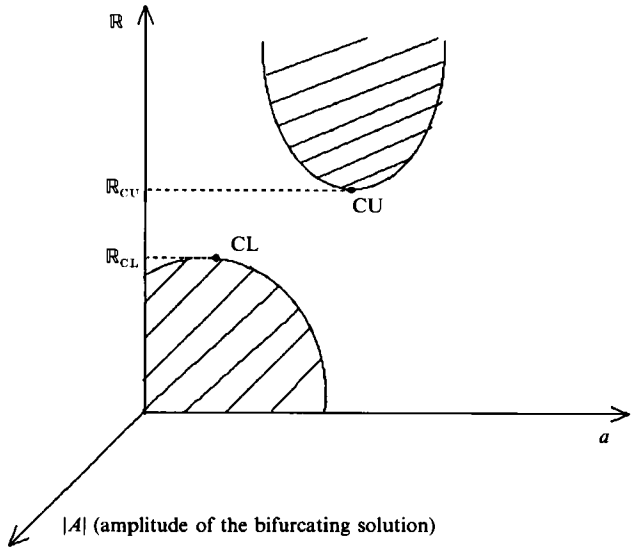

FIGURE 5. Neutral curves for the rare set of conditions in which PCAF can be stable. Bifurcation theory applies for $\mathbb{R}$ near to $\mathbb{R}_{CU}$ or $\mathbb{R}_{CL}$. When $\mathbb{R} > \mathbb{R}_{CU}$ and $|A| > 0$ then the flow is supercritical. When $\mathbb{R} < \mathbb{R}_{CL}$ and $|A| > 0$, then the flow is supercritical (the shaded regions are supercritical). When $\mathbb{R}_{CL} < \mathbb{R} < \mathbb{R}_{CU}$ and $|A| > 0$, the flow is subcritical.

The lower branch of the neutral curve for $J^* = 1$ has a region in the neighbourhood of $(\alpha, \mathbb{R}(\alpha)) = (0, \mathbb{R}(0))$ in which the analysis of long waves may be relevant. In the case of very long waves, it may be impossible to obtain an amplitude equation of the Ginzburg–Landau type. The critical wavenumber at the nose of the neutral curve tends to zero so that the wave you are supposed to modulate is already hugely long. (We are indebted to A. Frenkel for this remark. He noted that to have a Ginzburg–Landau equation, the sideband width $\Delta\alpha$ ought to be small relative to the wavenumber α on which it is centred.) There are other types of lubrication-like approximations describing waves of slow variation rather than the slowly varying envelope of modulated waves as in the Ginzburg–Landau equation. In fact Frenkel *et al.* (1987) derived an amplitude equation of the Kuramoto–Sivashinsky type from an analysis of long waves. Frenkel (private communication) found a condition in which the motions of the core and of the annulus can be coupled in the Kuramoto–Sivashinsky system leading to an additional linear term which dispersed and dissipates waves. A clear exposition of this work, based on a systematic expansion in powers of a small parameter together with numerical solutions of the Kuramoto–Sivashinsky–Frenkel equation, has been given by Papageorgiou, Maldarelli & Rumschitzki (1990).

We are concerned that the neglect of inertia $\rho(\boldsymbol{u}\cdot\nabla)\boldsymbol{u}$ in nonlinear theories for long waves can lead to large errors in the case when the wavenumber $\tilde{\alpha}$ of the maximum growth rate is bounded strictly away from zero. A monochromatic linear wave proportional to $\exp[i\tilde{\alpha}(x-ct)]$ undergoes repeated multiplication leading to rapid growth of higher harmonics, which eventually may be cut off by dispersion and dissipation. This type of effect is removed from the nonlinear long-wave theories by assumption.

6. Small capillary numbers

When the capillary parameter J^* is small, the maximum growth rate for capillary instability cannot be greatly different from the value $\alpha = 0$ which maximizes $\mathbb{R}(\alpha)$ on the lower branch of the neutral curve shown in figure 3. We have selected the value $J^* = 1$ to represent weak surface tension. Our results are contained in the coefficients displayed in tables 2–5 and in figure 3. Tables 2–4 are for $a = 1.25$, corresponding to water/oil volume ratio $V_w/V_o = a^2 - 1 = 0.5025$. The coefficients of the Ginzburg–Landau equations in the case in which the densities of the oil and the water are the same, $\zeta_2 = 1$, are exhibited in table 2. We know from energy analysis of the linear problem that PCAF in the region above the upper branch of the neutral curve is unstable to interfacial friction (see HJ, BCJ). We expect that wavy core flow will arise from this instability. The entries in table 2 show that the bifurcating waves are supercritical when the viscosity of the lubricating annulus fluid is close to that of the core fluid, $m \geqslant 0.85$, and subcritical when $m \leqslant 0.8$. Stable small-amplitude shear waves are expected in the supercritical case and something else far from PCAF, perhaps large waves, in the subcritical case. Small viscosity difference can lead to stable wavy flow at the interface.

Turning next to the lower branch of the neutral curve, which is prey to modified capillary instability, we note that the bifurcation is supercritical when the viscosity ratio $\mu_2/\mu_1 = m \geqslant 0.7$ and subcritical when $m \leqslant 0.5$. We expect to see small-amplitude capillary waves in the supercritical case. This can be interpreted to mean that linear capillary instability is nonlinearly shear stabilized when the viscosities of the fluids are close, $m \geqslant 0.7$. The flows which bifurcate subcritically ($m \leqslant 0.5$) should be far from PCAF. These more viscous cores probably break into slugs or bubbles far from PCAF connected by thin threads. The results in table 2 indicate that when the densities of the fluids are matched, a large viscosity difference leads to subcritical bifurcation while a small viscosity difference can result in supercritical bifurcation.

We study next the effects of changing the density of the lubricant for the same fixed $a = 1.25$. If the lubricant is heavier than the core, say water and oil, $\zeta_2 > 1$. Can we change the nature of the bifurcations, i.e. change the dynamics of lubrication, by varying ζ_2? Table 3 shows that for fluids with a viscosity ratio $\mu_2/\mu_1 = m = 0.7$, the bifurcation of the upper branch for $\zeta_2 = 1$ can be changed from subcritical to supercritical by increasing the density ratio to $\zeta_2 = 1.2$. We can stabilize small-amplitude bifurcating waves driven by interfacial friction by increasing the density of the lubricant. The change of density does not destabilize the supercritical bifurcating solution on the lower branch. Table 4 gives results for a smaller viscosity ratio $m = 0.5$. The same disposition of bifurcations holds also when $m = 0.2$. The only difference is that the wavy solutions below the lower branch of the neutral curve are all stable when the viscosity ratio is large, $m = 0.7$ and are all unstable when $m = 0.5$ and $m = 0.2$. These results suggest that for a given surface tension, the bifurcation of the upper branch is sensitive to changes in the density ratio, while the lower branch is sensitive to changes of the viscosity ratio, but not to changes of the density ratio.

In table 5 we look at fluids with a viscosity ratio $m = 0.5$ for the effects of varying density ratios ζ_2. The difference here is that there is much less water: $a = 1.1$ and water to oil volume ratio $V_w/V_o = a^2 - 1 = 0.21$; there is five times more oil than water. This is a thin lubricating layer. The bifurcation of the periodic solution from the lower branch of the neutral curve is subcritical for ζ_2 between 0.5 and 1.6, as in the case $a = 1.25$. The bifurcation of a periodic solution from the upper branch of the

neutral curve can be changed from subcritical to supercritical by increasing the density of the lubricant. However, the transition density ratio for $a = 1.1$ occurs between $\zeta_2 = 1.4$ and $\zeta_2 = 1.5$, a larger transition ratio than for $a = 1.25$, $m = 0.5$, which is between $\zeta_2 = 1.0$ and $\zeta_2 = 1.2$ (see table 4). Suppose the density ratio of the fluids is between 1.2 and 1.5, $1.2 \leqslant \zeta_2 \leqslant 1.5$, and the viscosity ratio is $m = 0.5$. If the lubricating layer is relatively thick, $a = 1.25$, then the upper branch will bifurcate supercritically. However, if the lubricating layer is thin, say $a = 1.1$, then the upper branch will bifurcate subcritically. This indicates some kind of nonlinear break-down of the 'thin-layer effect'. In order to achieve a linearly stable core–annular flow, we need to have a thin lubricating layer. However, if the layer is too thin, the bifurcation of the upper branch will become subcritical. The exact physical implication of this subcritical bifurcation is not clear to us. However, in our experiments (BCJ), in a region where the superficial oil velocity is large and superficial water velocity is relatively small, corresponding to very small values of a, oil sticks to the pipe wall.

The role density difference plays in the stability of core–annular flow is interesting. The effects of density difference on the neutral stability curves of core–annular flow were studied in CBJ. The calculations of CBJ as well as the weakly nonlinear ones presented here show that the upper branch of the neutral curves are more sensitive to the changes of density ratio ζ_2 than the lower branch. For the upper branch, the Reynolds number is large and the effect of the effective gravity $[\![\zeta]\!]\,\mathbb{R}_g$ is negligible. The only place that the density ratio ζ_2 enters into the equations is through the jump in the perturbation pressure in the normal stress balance equation at the interface, (2.8). Relatively small changes in ζ_2 can cause a large perturbation of the pressure jump when the Reynolds number is large. This changes the stability of the upper branch considerably. When the Reynolds number is large, the pressure jump is basically equal to the jump in the inertia of the fluids which is large in this case. On the other hand, when the Reynolds number is small, density stratification manifests itself mainly through the effective gravity term $[\![\zeta]\!]\,\mathbb{R}_g$ in the basic flow. This term is not too large for the small pipes we have considered and the change of the lower branch is relatively small for the moderate changes in ζ_2.

We have also computed a few cases of up-flow, for $a = 1.1$, with $\mathbb{R}_g = -0.5$. After comparing these results with relevant entries in the previous tables, we found that there are only slight changes in the values of coefficients and the type of bifurcations remain the same for both upper branch and lower branch. This is expected for the case of not too large value of $|\mathbb{R}_g|$ and fixed value of a. Effective gravity $[\![\zeta]\!]\,\mathbb{R}_g$ has little effect on the stability, and particularly for the upper branch, there is almost no difference between up and down flows for both the neutral curves and bifurcations. For the lower branch, there is a slight shift of the neutral curves between the up and down flows, but the type of bifurcation is not affected. The large differences between up and down flows at moderate flow rates observed in experiments are due to the accumulation of oil in down flow and its depletion in up flow due to buoyancy. The water fraction is therefore greater and a is larger in up than in down flow.

7. Large capillary numbers

As the surface tension parameter J^* is increased, the wavenumber corresponding to the most unstable mode of the lower branch tends to the capillary limit $\alpha = 0.69$. CBJ showed that linearly stable CAF is possible only when the lubricating fluid is heavy, ζ_2 is large enough. The neutral curve for $a = 1.3$, $m = 0.5$, $J^* = 2000$, $\mathbb{R}_g = 0.5$ and $\zeta_2 = 1.2$ is shown in figure 4. For this set of parameters a, m, J^*, $\mathbb{R}_g$,

linearly stable CAF is only possible when $\zeta_2 \geqslant 1.2$. A heavy lubricant will stabilize capillary instability and the critical Reynolds number below which the flow is unstable to capillarity is decreased as ζ_2 is increased. However, increasing the density of the lubricant does not appear to change the nature of the bifurcation from the capillary branch, which is subcritical at least for the case $a = 1.3$, $m = 0.5$ and $J^* = 2000$ which we calculated. The subcritical bifurcation here may lead to the capillary break-up of the oil core and the formation of oil slugs and bubbles. Bifurcations from the upper branch when $(a, m, J^*) = (1.3, 0.5, 2000)$ are always supercritical, leading to the finite travelling waves at the interface.

The second example of large capillary number is exhibited in table 6 for the parameters $a = 1.1$, $m = 0.5$, $J^* = 2000$ and $\mathbb{R}_g = 0.5$. Linearly stable CAF is possible for a much wider range of ζ_2 because of the stabilization effect of the thin lubricating layer. However, the bifurcation of the capillary branch remains subcritical for all the density ratios considered. These results for $J^* = 2000$ and those for $J^* = 1$ show that the bifurcation of the lower branch is insensitive to the changes in density difference and water fraction. For the upper branch, from table 6(*a*), we see that there is a range of density ratios within which the bifurcation of the upper branch is subcritical. Outside of this range, i.e. for small and large density ratios, the bifurcation becomes supercritical. This result also holds when $J^* = 1$, as shown in §6, but the subcritical range is different. The breakdown of 'thin layer effect' for $J^* = 1$ also occurs for $J^* = 2000$.

How do changes in the viscosity ratio m change the bifurcations of core–annular flows when J^* is large? Table 7 gives results for $a = 1.1$, $m = 0.9$, $J^* = 2000$, $\mathbb{R}_g = 0.5$ and down-flow. The remarkable difference between $m = 0.9$ and $m = 0.5$ is that for the smaller viscosity stratification $m = 0.9$, the lower capillary branch bifurcates supercritically for all the density ratios considered, even for lighter lubricant, $\zeta_2 < 1$. This means that finite-amplitude capillary waves are saturated nonlinearly by the action of a small viscosity difference, m near one. This nonlinear saturation by small viscosity difference also occurs when J^* is small (see §6). For the upper branch, there is still a range of density ratios within which the bifurcation is subcritical, as in the case of weak capillarity.

8. Experiments

In the somewhat restricted situation of Hopf bifurcation of strictly periodic waves at a simple eigenvalue, we could say that the supercritical waves are stable whilst the subcritical waves are unstable. To compare bifurcation analysis with experiments, we must first identify a flow with a critical Reynolds number $\mathbb{R}_c$. There are then upper and lower critical values of Reynolds number, $\mathbb{R}_{cU}$ and $\mathbb{R}_{cL}$ (see figure 5). If the operating Reynolds number $\mathbb{R}$ is in a region of instability of PCAF near criticality, then supercritical bifurcating solutions are in this same region of instability of PCAF. Under restrictive hypotheses, the supercritical bifurcating solution is stable. We say that bifurcation theory is consistent with experiments when the observed supercritical solution is just a small perturbation of PCAF (we would need to compare details of the bifurcated solution with experiments to test the theory, and we have not done this). On the other hand, if the bifurcation is subcritical when $\mathbb{R}$ is in the unstable region for PCAF (shaded region in figure 5), then the bifurcating solution is unstable when its amplitude is small, but may recover stability for large amplitudes. In this case the observed flows would be far from PCAF. If $\mathbb{R}$ is in a region of stability of PCAF, $\mathbb{R}_{cL} < \mathbb{R} < \mathbb{R}_{cU}$, and both bifurcations are supercritical,

we might expect to see stable PCAF, stable both to small and finite disturbances. If, on the other hand, one or both bifurcations are subcritical and $\mathbb{R}_{cL} < \mathbb{R} < \mathbb{R}_{cU}$, then the conclusion of the bifurcation theory is ambiguous. Without ambiguity, we may conclude that if a flow different to stable PCAF is seen in the linear stable range, then one or both bifurcations should be subcritical with large deviations (with an ambiguous 'large') from PCAF.

In table 8, we have compared bifurcation theory with experiments. The comparisons exhibited in rows 1 and 2 can be said to show agreements between theory and experiments. Less can be concluded from rows 3–7, but in all cases, there is no obvious inconsistency between experiments and bifurcation theory.

We wish to draw attention to a possible interpretation of bamboo waves as a structure far from PCAF. When the bamboo waves are large, they are clearly far from PCAF. In one interpretation, bamboo waves arise from shear stabilization of capillary instability which in pure form leads to spheres of oil, far from PCAF. There is no stable capillary figure close to a cylinder.

We turn next to a discussion of theory and experiments in which the entries in table 8 are explained in a wider context. We first consider the experiment labelled as 2 in figure 3 of the paper by Charles *et al.* (1961) (reproduced as figure 1 in PCJ and figure 6 in HJ), one sees a slightly perturbed PCAF which is labelled as 'oil in water concentric'. The neutral curve for this case is shown as figure 13 in PCJ. The operating condition, $a = 1.21$, $J^* = 2102$, $m = 0.0532$, $\mathbb{R} = 138.6$, is just above the nose $(\alpha_c, \mathbb{R}_c) = (2.24, 138.2)$ of the upper neutral curve, hence PCAF is linearly unstable. For this case the coefficients of the amplitude equation (3.17) are

$$C_d = -1.3967, \quad C_n = -0.02393, \quad \text{sign}\,(l_r) = +1.$$

Since $l_r > 0$, the bifurcation is supercritical and only a small perturbation of PCAF is expected and is realized. The remaining ten cases corresponding to figure 3 of Charles *et al.* (1961), are either always unstable or with operating conditions (operating Reynolds numbers) far away from the critical conditions (see PCJ and Chen (1990) for the neutral curves). Thus bifurcation analysis cannot be applied.

The analysis of §§6, 7 may be applied to situations when the two fluids involved have similar physical properties. CBJ designed an experiment to test the validity of the linear theory. The fluids and the size of pipe were chosen with the guidance of the linear theory. They successfully realized globally stable perfect core–annular flow in the free-fall apparatus and showed perfect agreement between linear theory and their experiment. The neutral curve for this experiment is given in figure 20 of CBJ. The experiment falls in the linearly stable region and is not too far away from the critical condition of the lower branch. After converting the parameters to the ones used in the present paper, we have, for the experiment,

$$a = 1.86, \quad m = 0.33, \quad \zeta_2 = 1.4, \quad J^* = 2.26, \quad \mathbb{R}_g = 21.31, \quad \mathbb{R} = 8.22.$$

The bifurcation near the critical state of the lower branch, $(\alpha_c, \mathbb{R}_c) = (0.04, 6.31)$, is supercritical:

$$C_d = 89.65, \quad C_n = 21.31, \quad \text{sign}\,(l_r) = +1.$$

The upper branch, although far away with $(\alpha_c, \mathbb{R}_c) = (0.5, 153.0)$, also bifurcates supercritically. Perfect core–annular flow was observed in the experiment and it agrees with both the linear and nonlinear theory.

The difficulties one encounters when applying the above bifurcation theory to the

Experiment	Operating $\mathbb{R}$	sgn $(l_r)_U$	sgn $(l_r)_L$	Observations and comments
Charles *et al.* No. 2	$\mathbb{R} > \mathbb{R}_{cU}$	+1		The bifurcation is supercritical and the flow is near to PCAF
CBJ Free fall	$\mathbb{R}_{cL} < \mathbb{R} < \mathbb{R}_{cU}$	+1	+1	PCAF is observed. Perfect agreement between experiments and linear and nonlinear theory
BCJ E2, up flow	$\mathbb{R} > \mathbb{R}_{cU}$	−1		Bamboo waves, a structure far from PCAF
BCJ F1, up-flow	$\mathbb{R} > \mathbb{R}_{cU}$	−1		Oil sticks to the pipe wall
BCJ No. 2, down-flow	$\mathbb{R}_{cL} < \mathbb{R} < \mathbb{R}_{cU}$	−1	−1	Intermittent corkscrew waves are observed
BCJ No. 3, down-flow	$\mathbb{R}_{cL} < \mathbb{R} < \mathbb{R}_{cU}$	−1	−1	Intermittent corkscrew waves are observed
BCJ No. 4, down-flow	$\mathbb{R} \gg \mathbb{R}_{cU}$	+1		Disturbed bamboo waves, perhaps not too far from PCAF are observed

TABLE 8. Comparison of bifurcation theory and experiments. Among many experiments, there are only a small number to which the Ginzburg–Landau theory might apply. They are listed in this table. sgn $(l_r) = +1$ for supercritical, sgn $(l_r) = -1$ for subcritical bifurcations. Subscripts U and L are referred to upper and lower branch respectively.

practical situations of lubricated pipelining lie in the fact that, when the viscosity ratio of water to oil, $m = \mu_2/\mu_1$, is very small, say m of order 10^{-5} which is typical for crude oil and water, PCAF is always linearly unstable and thus there is no critical state for bifurcation analysis. This restriction severely limited the parameter ranges to which we could apply such analysis.

The experiments of BCJ revealed many interesting features of nonlinear waves in lubricated pipelining. For these experiments, we have

$$m = 1.66 \times 10^{-3}, \quad \zeta_2 = 1.0994, \quad J^* = 0.1019, \quad \mathbb{R}_g = 2.4.$$

For this value of m, linearly CAF can be obtained only when a is very small (say $a < 1.15$). The flow charts in BCJ show how different flow regimes change with respect to the superficial velocities of water and oil, V_w, V_o. In the up-flow chart, there is a region in the V_w, V_o plane called 'wavy CAF', which corresponds to the bamboo waves observed (see figure 1). For the points marked 1–9, and D2, E3 in the bamboo wave regime (BCJ), the upper and lower neutral curves are connected and they are linearly unstable at all Reynolds numbers. This is because of the large values of a for these points. For point E2, $a = 1.12, \mathbb{R} = 1.2283$. The upper and lower branches of the neutral curves are separated. The experimental line $\mathbb{R} = 1.2283$ is cutting through the upper branch, linearly unstable and is not too far away from the nose of the neutral curve $(\alpha_c, \mathbb{R}_c) = (2.41, 0.501)$. The bifurcaton at this point is found to be subcritical with

$$C_d = 0.9623, \quad C_n = -0.9657, \quad \text{sign}\,(l_r) = -1.$$

The subcritical bifurcation indicates that in order to achieve the experimentally observed stable bamboo waves at E2, higher-order theory is needed.

The examples discussed above show that the current lowest-order bifurcation theory is hopeless for the prediction of bamboo waves observed by BCJ, either because the corresponding linear theory predicts linear instability for all Reynolds numbers, or because of the subcriticality of the bifurcation. for the latter case, we may supplement a higher-order theory. Nevertheless, the above examples suggest that bamboo waves are flows far from PCAF and fully numerical simulations may be required for their characterizations.

The flow regime called 'oil sticking on the wall' in the up-flow chart is a region where V_w is small and V_0 is large. In this region, there is little water in the pipe and thus the value of a is small. We found that for these small values of a, the upper and lower branch of the neutral curves are separated, owing to the strong stabilization of the thin lubricating layer ('thin-layer effect'). The experimental lines $\mathbb{R} = \mathbb{R}_E$ cut through the upper branch. However, the bifurcations of the upper branch are found to be all subcritical. This is the nonlinear break-down of the 'thin-layer effect' discussed in §6. An example in this region is the point F1, where $a = 1.03$, $\mathbb{R} = 2.2838$. The nose of the upper branch is $(\alpha_c, \mathbb{R}_c) = (12.0, 2.04)$ and we have a subcritical bifurcation with

$$C_d = -0.1479, \quad C_n = -0.7556, \quad \text{sign}\,(l_r) = -1.$$

Whether these subcritical bifurcations correlate to the losses of lubrication observed in the experiments remains to be resolved, either by higher-order theory or numerical solution. Obviously the phenomena observed in the experiments are very nonlinear.

Turning now to the down-flow chart of BCJ. The points 2 and 3 fall in a region called 'disturbed CAF', corresponding to 'corkscrew' waves as in figure 2. The linear theory predicts that 2 and 3 are linearly stable to infinitesimal disturbances, axisymmetric and non-axisymmetric. The bifurcations of the upper and lower branches are all subcritical. It is obvious that these 'corkscrew' waves are non-axisymmetric and due to finite non-axisymmetric disturbances which are not considered in this paper.

Point 4 in the down-flow chart falls in a region called 'disturbed CAF', which corresponds to axisymmetric, very short stem bamboo waves. For point 4, $a = 1.09$, $\mathbb{R} = 9.59$, the upper and lower branch are separated, and $\mathbb{R} = 9.59$ cuts through the upper branch. In this case, the bifurcation at the nose of upper branch $(\alpha_c, \mathbb{R}_c) = (3.6, 1.36)$ is supercritical with

$$C_d = 0.6590, \quad C_n = -0.5718, \quad \text{sign}\,(l_r) = +1.$$

However, the experimental point $\mathbb{R} = 9.59$ is far away from the nose and the information on the bifurcation at the nose may be not relevant to the observed equilibrium waves.

A summary of the results testing the bifurcation theory is given in table 8. It is evident from the above discussions that the usefulness of the bifurcation analysis is very restricted. For the situations of practical interest, $m \ll 1$, the bifurcation analysis is either not applicable or fails to provide useful information relevant to the experimentally observed phenomena. On the other hand, in all these cases we have obtained useful information from the study of the linear theory of stability. It seems to us that, unlike linear theory, weakly nonlinear theory is valid only in a too narrowly defined set of conditions to be of much use in our problem. Perhaps direct numerical approaches have more to offer.

9. Summary and discussion

1. There are regions of parameter space in which PCAF is possible. For these parameters we can write two Ginzburg–Landau equations, one near the minimum point of the upper branch and another near the maximum point of the lower branch. At the upper branch, PCAF loses stability to waves generated by interfacial friction. At the lower branch PCAF loses stability to capillary waves.

2. There are yet more regions of parameter space in which PCAF is not possible. For these cases, bifurcation analysis is not applicable.

3. The singular value decomposition is a useful numerical method for computing the coefficients of the Ginzburg–Landau equation.

4. The stability of wavy flows near the upper branch of the neutral curve can be controlled by varying the density ratio ζ_2. For example, when the other parameters are fixed we can choose a best $\zeta_2 = \hat{\zeta}_2$ to maximize the minimum critical value $\mathbb{R}_U(\zeta_2)$ of the linear theory on the upper branch of the neutral curve (CBJ). The bifurcation of waves from the upper branch $\mathbb{R}_U(\zeta_2)$ of the neutral curve will be supercritical if ζ_2 is large enough. For smaller values of ζ_2 the bifurcation is subcritical.

5. The lower branch is less sensitive to changes in ζ_2 than the upper branch. The critical Reynolds number above which down-flow is linearly stable decreases with increasing ζ_2. In up-flow, smaller values of ζ_2 lead to larger regions of linear stability (CBJ). The bifurcation of the lower branch is controlled by the viscosity difference and surface tension. Changes of ζ_2 do not change the directions of bifurcation of the lower branch.

6. The viscosity ratio, m, plays a key role in determining both the linear and nonlinear stability of core–annular flows. When m is small, linear stable PCAF cannot be achieved (PCJ, HLJ). Stable PCAF can be achieved only when the viscosity difference $1-m$ is small.

7. Other things being equal, the linear theory tells us that we will get larger intervals of the Reynolds number in which PCAF is stable if the lubricating layer is thin, $a \to 1$. We can say that this stability will be realized practically even when PCAF is unstable, if the bifurcating solutions of small amplitude are stable. This means that a robust form of lubricated pipelining with thin lubricating films is expected when the bifurcations are supercritical, but nonlinear failures may occur when the bifurcations are subcritical. We have in fact found that subcritical bifurcations for thin film solutions which bifurcate from the upper branch and these solutions lie in a region of thin film parameter space in which a failure of lubrication does occur (see BCJ). On the other hand, there are cases for which increasing the thickness of the lubricating layer can change subcritical bifurcation to supercritical bifurcation.

8. When the flows are slight perturbations of PCAF, experiments agree perfectly with both linear and nonlinear theories. One example is experiment 2 of Charles *et al.* (1961) where nearly perfect core–annular flow is observed. The operating Reynolds number of the experiment is slightly above the nose of the upper branch of the neutral curve where the bifurcation is found to be supercritical. An even more convincing example is the free-fall experiment of CBJ in which PCAF is predicted and observed.

9. The finite-amplitude bamboo waves observed by BCJ are evidently too far from PCAF to be described by our Ginzburg–Landau equation. In most cases encountered in the experiments of BCJ, the bifurcation theory cannot be applied because the corresponding PCAF is linearly unstable at all Reynolds numbers. In other cases, the

experimental Reynolds numbers cut through the upper branch of the neutral curves, but the bifurcations near the nose of the upper branch are subcritical. These results suggest that bamboo waves and other flows far from PCAF perhaps may be best treated by direct numerical methods.

This work was supported by the Department of Energy; the US Army Research Office, Mathematics; the National Science Foundation and the Minnesota Supercomputer Institute. K.C. wishes to thank Professor P. Huerre for his advice. We are also grateful to the suggestions and comments of the editor and the referees.

Appendix

The interfacial operators corresponding to equation (3.13) are defined as:

$$\mathscr{L}_{i1}(\psi_l,\delta)=\delta_t+W(1)\,\delta_x+\psi_x,\quad \mathscr{Q}_{i1}(\psi_l,\delta)=-\{W'(1)\,\delta\delta_x+\delta_x\psi_r+\delta(\psi_{rx}-\psi_x)\},$$

$$\mathscr{C}_{i1}(\psi_l,\delta)=-\{\tfrac{1}{2}W''(1)\,\delta^2\delta_x+\delta\delta_x(\psi_{rr}-\psi_r)+\delta^2(\tfrac{1}{2}\psi_{rrx}-\psi_{rx}+\psi_x)\};$$

$$\mathscr{L}_{i2}(\psi)=\psi_x,\quad \mathscr{Q}_{i2}(\psi_1,\psi_2,\delta)=-\delta[\![\psi_{rx}]\!],$$

$$\mathscr{C}_{i2}(\psi_1,\psi_2,\delta)=-\tfrac{1}{2}\delta^2[\![\psi_{rrx}]\!];\quad \mathscr{L}_{i3}(\psi,\delta)=W'(1)\,\delta+\psi_r,$$

$$\mathscr{Q}_{i3}(\psi_1,\psi_2,\delta)=-\tfrac{1}{2}\delta^2[\![W''(1)]\!]-\delta[\![\psi_{rr}-\psi_r]\!],$$

$$\mathscr{C}_{i3}(\psi_1,\psi_2,\delta)=-\tfrac{1}{6}\delta^3[\![W'''(1)]\!]-\delta^2[\![\tfrac{1}{2}\psi_{rrr}-\psi_{rr}+\psi_r]\!];$$

$$\mathscr{L}_{i4}(\psi,\delta)=\psi_{rr}-\psi_r-\psi_{xx}+W''(1)\,\delta,$$

$$\mathscr{Q}_{i4}(\psi_1,\psi_2,\delta)=-[\![m\{\tfrac{1}{2}\delta^2W'''(1)+\delta(\psi_{rrr}-\psi_{rr}+\psi_r-\psi_{rxx})+2\delta_x(-2\psi_{rx}+\psi_x)\}]\!],$$

$$\mathscr{C}_{i4}(\psi_1,\psi_2,\delta)=-[\![m\{\tfrac{1}{6}\delta^3W''''(1)-\delta\delta_x^2\,W''(1)+\delta^2(\tfrac{1}{2}\psi_{rrrr}-\tfrac{1}{2}\psi_{rrr}+\psi_{rr}-\psi_r$$
$$-\tfrac{1}{2}\psi_{rrxx})-\delta_x^2(\psi_{rr}-\psi_r-\psi_{xx})+2\delta\delta_x(-2\psi_{rrx}+\psi_{rx}-\psi_x\}]\!];$$

$$\mathscr{L}_{i5}(\psi,\delta)=\zeta\{\psi_{rt}+W(1)\,\psi_{rx}-W'(1)\,\psi_x\}+\frac{m}{\mathbb{R}_1}\{-\psi_{rrr}+\psi_{rr}-\psi_r$$
$$-3\psi_{rxx}+2\psi_{xx}-2\delta_{xx}\,W'(1)\},$$

$$\mathscr{Q}_{i5}(\psi_1,\psi_2,\delta)=-[\![\zeta\{\delta[\psi_{rrt}-\psi_{rt}+W(1)\,(\psi_{rrx}-\psi_{rx})+(W'(1)-W''(1)\,\psi_x]$$
$$-\delta_x[\psi_{xt}+W(1)\,\psi_{xx}]+[-\psi_x(\psi_{rr}-\psi_r)+\psi_r\psi_{rx}]\}$$
$$+\frac{m}{\mathbb{R}_1}\{-\delta[-\psi_{rrrr}+2\psi_{rrr}-3\psi_{rr}+3\psi_r-3\psi_{rrxx}+5\psi_{rxx}$$
$$-4\psi_{xx}-2\delta_{xx}\,W''(1)]-2\delta_{xx}[\psi_{rr}-\psi_r-\psi_{xx}]+\delta_x[-3\psi_{rrx}$$
$$+5\psi_{rx}-4\psi_x+3\psi_{xxx}-2\delta_x\,W''(1)]\}]\!]+\frac{J^*}{a\mathbb{R}_1^2}\delta_x(\delta_{xx}-2\delta),$$

$$\mathscr{C}_{i5}(\psi_1,\psi_2,\delta)=-[\![\zeta\{\delta^2[\tfrac{1}{2}\psi_{rrrt}-\psi_{rrt}+\psi_{rt}+W(1)\,(\tfrac{1}{2}\psi_{rrrx}-\psi_{rrx}+\psi_{rx})$$
$$+W'(1)\,(\tfrac{1}{2}\psi_{rrx}-\psi_x)+W''(1)\,(-\tfrac{1}{2}\psi_{rx}+\psi_x)-\tfrac{1}{2}W'''(1)\,\psi_x]$$
$$+\delta[\psi_x(-\psi_{rrr}+3\psi_{rr}-3\psi_r)+\psi_r(\psi_{rrx}-\psi_{rx})]$$
$$-\delta\delta_x[\psi_{rxt}-\psi_{xt}+W(1)\,\psi_{rxx}+(W'(1)-W(1))\,\psi_{xx}]$$
$$+\delta_x[\psi_x(\psi_{rx}-\psi_x)-\psi_r\psi_{xx}]\}$$
$$+\frac{m}{\mathbb{R}_1}\{\delta^2[-\tfrac{3}{2}\psi_{rrrxx}+4\Psi_{rrxx}-7\psi_{rxx}+6\psi_{xx}-\delta_{xx}\,W'''(1)$$

$$
\begin{aligned}
&-\tfrac{1}{2}\psi_{rrrrr}+\tfrac{3}{2}\psi_{rrrr}+\tfrac{17}{2}\psi_{rrr}+6\psi_{rr}-6\psi_r]\\
&-2\delta\delta_x[\psi_{rrr}-2\psi_{rr}+2\psi_r-\psi_{rxx}+\psi_{xx}]\\
&+4\delta_x\delta_{xx}[2\psi_{rx}-\psi_x]+6\delta_x^2\delta_{xx}W'(1)\\
&+\delta\delta_x[-3\psi_{rrrx}+8\psi_{rrx}-14\psi_{rx}+12\psi_x\\
&-3\psi_{xxx}+3\psi_{rxxx}-2\delta_x W''(1)]\\
&+2\delta_x^2[-\psi_{rrr}+2\psi_{rr}-2\psi_r+3\psi_{rxx}-2\psi_{xx}]\}]\\
&+\frac{J^*}{a\mathbb{R}_1^2}(3\delta_x\delta_{xx}^2-\tfrac{3}{2}\delta_{xxx}\delta_x^2-\tfrac{1}{2}\delta_x^3-\delta\delta_x\delta_{xx}+3\delta^2\delta_x).
\end{aligned}
$$

REFERENCES

Bai, R., Chen, K. & Joseph, D. D. 1991 Lubricated pipelining: stability of core–annular flow. Part 5. Experiments and comparison with theory. *J. Fluid Mech.* (submitted).

Bretherton, C. S. & Spiegel, E. A. 1983 Intermittency through modulational instability. *Phys. Letts.* **96** A (3), 152–156.

Charles, M. E., Govier, G. W. & Hodgson, G. W. 1961 The horizontal pipeline flow of equal density oil–water mixtures. *Can. J. Chem. Engng* **39**, 17–36.

Chen, K. 1990 Lubricated pipelining: stability of core–annular flows. PhD thesis, University of Minnesota.

Chen, K., Bai, R. & Joseph, D. D. 1990 Lubricated pipelining. Part 3. Stability of core–annular flow in vertical pipes. *J. Fluid Mech.* **214**, 251–286.

Chen, K. & Joseph, D. D. 1990 Application of the singular value decomposition to the numerical computation of the coefficients of amplitude equations and normal forms. *Appl. Num. Math.* **6**, 425–430.

Craik, A. D. D. 1983 *Wave Interactions and Fluid Flows.* Cambridge University Press.

Davey, A., Hocking, L. M. & Stewartson, K. 1974 On the nonlinear evolution of three-dimensional disturbances in plane Poiseuille flow. *J. Fluid Mech.* **63**, 529–536.

Frenkel, A. L., Babchin, A. J., Levich, B. G., Shlang, T. & Sivashinsky, G. I. 1987 Annular flows can keep unstable films from breakup: Nonlinear saturation of capillary instability. *J. Colloid Interface Sci.* **115**, 225–233.

Ginzburg, V. L. & Landau, L. D. 1950 *Sov. Phys., J. Exp. Theor. Phys.* **20**, 1064.

Golub, G. H. & Van Loan, C. F. 1983 *Matrix Computations.* Baltimore: Johns Hopkins University Press.

Herbert, T. 1980 Nonlinear stability of parallel flows by higher order amplitude expansions. *AIAA J.* **18**, 243–248.

Hocking, L. M. & Stewartson, K. 1972 On the nonlinear response of a marginally unstable plane parallel flow to a two-dimensional disturbance. *Proc. R. Soc. Lond.* A **326**, 289–313.

Hocking, L. M., Stewartson, K. & Stuart, J. T. 1972 A nonlinear instability burst in plane parallel flow. *J. Fluid Mech.* **51**, 705–735.

Holmes, P. 1986 Spatial structure of time-periodic solutions of the Ginzburg–Landau equation. *Physica* **23** D, 84–90.

Hu, H. & Joseph, D. D. 1989 Lubricated pipelining: stability of core–annular flow. Part 2. *J. Fluid Mech.* **205**, 359–396.

Hu, H., Lundgren, T. & Joseph, D. D. 1990 Stability of core–annular flow with a small viscosity ratio. *Phys. Fluids* A **2**, 1945–1954.

Joseph, D. D., Renardy, Y. & Renardy, M. 1984 Instability of the flow of immiscible liquids with different viscosities in a pipe. *J. Fluid Mech.* **141**, 319–345.

Joseph, D. D. & Sattinger, D. H. 1972 Bifurcating time periodic solutions and their stability. *Arch. Rat. Mech. Anal.* **45**, 79–109.

Moon, H. T. 1982 Transition to chaos in the Ginzburg–Landau equation. PhD thesis, University of Southern California.

MOON, H. T., HUERRE, P. & REDEKOPP, L. G. 1983 Transition to chaos in the Ginzburg–Landau equation. *Physica* **7D**, 135.

NEWELL, A. C. 1974 Envelope equations. In *Lectures in Applied Mathematics*, vol. 15, pp. 157–163.

NEWELL, A. C. 1985 *Solitons in Mathematics and Physics* (CBMS-NSF Regional Conference Series in Applied Mathematics, SIAM publication).

NEWELL, A. C., PASSOT, T. & SOULI, M. 1989 The phase diffusion and mean drift equations for convection at finite Rayleigh numbers in large containers I. Preprint.

NEWELL, A. C. & WHITEHEAD, J. A. 1969 Finite bandwidth, finite amplitude convection. *J. Fluid Mech.* **38**, 279–304.

PAPAGEORGIOU, D. T., MALDARELLI, C. & RUMSCHITZKI, D. S. 1990 Nonlinear interfacial stability of core annular film flows. *Phys. Fluids* A**2**, 340–352.

PREZIOSI, L., CHEN, K. & JOSEPH, D. D. 1989 Lubricated pipelining: stability of core–annular flow. *J. Fluid Mech.* **201**, 323–356.

REYNOLDS, W. C. & POTTER, M. C. 1967 Finite amplitude instability of parallel shear flow. *J. Fluid Mech.* **27**, 465–492.

SEGEL, L. A. 1969 Distance side-walls cause flow amplitude modulation of cellular convection. *J. Fluid Mech.* **38**, 203–224.

SEN, P. K. & VENKATESWARLU, D. 1983 On the stability of plane Poiseuille flow to finite-amplitude disturbances, considering the higher-order Landau coefficients. *J. Fluid Mech.* **133**, 179–206.

STEWARTSON, K. & STUART, J. T. 1971 A nonlinear instability theory for a wave system in plane Poiseuille flow. *J. Fluid Mech.* **48**, 529–545.